

# Bayesian inference on the Stiefel manifold

Vinayak Rao, Lizhen Lin, and David Dunson \*

## Abstract

The Stiefel manifold  $V_{p,d}$  is the space of all  $d \times p$  orthonormal matrices, and includes the  $d-1$  hypersphere and the space of all orthogonal matrices as special cases. It is often desirable to parametrically or nonparametrically estimate the distribution of variables taking values on this manifold. Unfortunately, the intractable normalizing constant in the likelihood makes Bayesian inference challenging. We develop a novel Markov chain Monte Carlo algorithm to sample from this doubly intractable distribution. By mixing the matrix Langevin with respect to a random probability measure, we define a flexible class of nonparametric models. Theory is provided justifying the flexibility of the model and its asymptotic properties, while we also extend the MCMC algorithm to this situation. We apply our ideas to simulated data and two real datasets, and also discuss how our sampling ideas are applicable to other doubly intractable problems.

**Keywords:** Density estimation; Dirichlet process; Doubly intractable; Matrix Langevin; MCMC; Mixture model; Orthonormal vectors; Stiefel manifold.

## 1 Introduction

Matrices with orthonormal columns play an important role in statistics, signal processing and machine learning, with applications ranging from studies of orientations of orbits of comets and asteroids to principal components analysis to the estimation of rotation matrices. Central to probabilistic models involving such matrices are probability distributions on the Stiefel manifold, the space of all  $d \times p$  orthonormal matrices. Popular examples of parametric distributions on the Stiefel manifold are the matrix von Mises-Fisher distribution (Khatrı and Mardia, 1977; Hornik and Grn, 2013) (also known as the matrix Langevin (Chikuse, 1993, 2003a, 2006)), and its generalization, the Bingham-von Mises-Fisher distribution (Hoff, 2009b). Bayesian inference for such distributions is difficult due to the intractable normalization constants in the likelihood function (such problems are called *doubly intractable* (Murray et al., 2006)).

One of our first contributions is to develop an exact MCMC sampling algorithm for the parametric matrix Langevin distribution. Our sampler is based on a representation of

---

\*Department of Statistical Science, Duke University, USA

the matrix Langevin distribution provided in Hoff (2009b), involving a rejection sampling scheme. Related ideas that exist in the literature (e.g. Adams et al. (2009)) do not exploit a simple independence property of the rejected variables in a rejection sampler, and are unnecessarily complicated. Directly applying the sampler of Adams et al. (2009) to our problem destroys certain conjugacy properties, and can lead to significant inefficiency.

By mixing the parametric kernel with a random probability measure, we extend our model to a class of flexible nonparametric models. Nonparametric inference on the Stiefel manifold has been limited to the estimation of Fréchet means (Bhattacharya and Bhattacharya (2012)). Model-based nonparametric inference has advantages, allowing the flexible accommodation of prior beliefs, and allowing inferences to adapt to the complexity of the data. We show that our nonparametric models have large support, and that the resulting posterior distributions are consistent. We generalize our proposed MCMC sampling algorithms to these nonparametric extensions as well.

Overall, our work develops theory and algorithms for parametric and nonparametric Bayesian inference on the Stiefel manifold, both of which are very underdeveloped. Depending on the application, our models can be used to characterize the data directly, or to describe latent components of a hierarchical model. Section 2 provides some details on the geometry of the Stiefel manifold. Section 3 introduces the matrix Langevin distribution, and takes a Bayesian approach to estimating its parameters. In Section 4, we describe the doubly-intractable nature of the problem, and develop a novel MCMC sampler for posterior inference, which we evaluate on a number of datasets in Section 5. Section 6 introduces a nonparametric extension of the matrix Langevin distribution, and is devoted to studying the theoretical support and asymptotic properties. We finish with more experiments in Section 7.

## 2 Geometry of the Stiefel manifold

The Stiefel manifold  $V_{p,d}$  is the space of all  $p$ -frames in  $\mathbb{R}^d$ , with a  $p$ -frame consisting of  $p$  ordered orthonormal vectors in  $\mathbb{R}^d$ . Writing  $M(d,p)$  for the space of all  $d \times p$  real matrices, and letting  $I_p$  represent the  $p \times p$  identity matrix, the Stiefel manifold can be represented as

$$V_{p,d} = \{X \in M(d,p) : X^T X = I_p\}. \quad (1)$$

The Stiefel manifold  $V_{p,d}$  has the  $d-1$  hypersphere  $S^{d-1}$  as a special case when  $p=1$ . When  $p=d$ , this is the space of all the orthogonal matrices  $O(d)$ .  $V_{p,d}$  is a Riemannian manifold of dimension  $dp - p - p(p-1)/2 = p(2d-p-1)/2$ . It can be embedded into the Euclidean space  $M(d,p)$  of dimension  $dp$  with the inclusion map as a natural embedding, and is thus a submanifold of  $\mathbb{R}^{dp}$ .

Let  $G \in V_{p,d}$ , and  $G_1$  be a matrix of size  $d \times (d-p)$  such that  $[G : G_1]$  is in  $O(d)$ , the group of  $d$  by  $d$  orthogonal matrices. The volume form on the manifold is  $\lambda(dG) = \wedge_{i=1}^p \wedge_{j=i+1}^d g_j^T dg_i$  where  $g_1, \dots, g_p$  are the columns of  $G$ ,  $g_{p+1}, \dots, g_d$  are the columns of  $G_1$  and  $\wedge$  represents the wedge product (Muirhead, 2005). If  $p=d$ , that is when  $G \in O(d)$ , one can represent  $\lambda(dG) = \wedge_{i < j} g_j^T dg_i$ . Note that  $\lambda(dG)$  is invariant under the left action of the orthogonal

group  $O(d)$  and the right action of the orthogonal group  $O(p)$ , and forms the Haar measure on the Stiefel manifold. For more details on the Riemannian structure of the Stiefel manifold, we refer to Edelman et al. (1998).

### 3 Bayesian inference for the matrix Langevin distribution

#### 3.1 The matrix Langevin distribution

Let  $X$  be a random variable on  $V_{p,d}$  distributed according to the matrix Langevin distribution. This has density  $P_{\text{ML}}$  with respect to the invariant Haar volume measure on  $V_{p,d}$  given by

$$P_{\text{ML}}(X|F) = \text{etr}(F^T X)/Z(F), \quad (2)$$

where the parameter  $F$  is a  $d \times p$  matrix. The normalization constant  $Z(F) = {}_0F_1(\frac{1}{2}d, \frac{1}{4}F^T F)$  is the hypergeometric function with matrix arguments, evaluated at  $\frac{1}{4}F^T F$  (Chikuse, 2003b). Let  $F = G\kappa H^T$  be the singular value decomposition (SVD) of  $F$ , where  $G$  and  $H$  are  $d \times p$  and  $p \times p$  orthonormal matrices, and  $\kappa$  is a diagonal matrix with positive elements. One can think of  $G$  and  $H$  as orientations, with  $\kappa$  controlling the concentration in the directions determined by these orientations. Large values of  $\kappa$  imply concentration along the associated directions, while setting  $\kappa$  to zero recovers the uniform distribution on the Stiefel manifold. It can be shown (Khatri and Mardia, 1977) that  ${}_0F_1(\frac{1}{2}d, \frac{1}{4}F^T F) = {}_0F_1(\frac{1}{2}d, \frac{1}{4}\kappa^T \kappa)$ , so that the normalization constant depends only on  $\kappa$ , and we write it as  $Z(\kappa)$ . The mode of the distribution is given by  $GH^T$ , and from the characteristic function of  $X$ , one can show  $E(X) = FU$ , where the  $(i, j)$ th element of the matrix  $U$  is given by

$$U_{ij} = 2 \frac{\partial \log {}_0F_1(\frac{1}{2}d, \frac{1}{4}F^T F)}{\partial (F^T F)_{ij}}.$$

Consider  $n$  observations  $X_1, \dots, X_n$  drawn i.i.d. from  $P_{\text{ML}}(X|F)$ . A simple approach to characterizing these observations is via a maximum likelihood estimate of the parameter  $F$  (Chikuse, 2003b, Section 5.2). By contrast, a Bayesian approach involves specifying a prior distribution for  $F$ , with inferences carried out based on the resulting posterior. Such an approach was followed in Camano-Garcia (2006) and Hoff (2009a); however, this is complicated by the fact that the normalization constant  $Z(\kappa)$  is difficult to evaluate. This results in what is called a doubly intractable distribution (Murray et al., 2006), where even characterizing the posterior distribution over  $\kappa$  via samples from a Markov chain Monte Carlo (MCMC) algorithm is intractable (see Section 4). Thus, Camano-Garcia (2006) keeps  $\kappa$  constant, while Hoff (2009a) uses a first-order Taylor expansion of the intractable term to run an approximate MCMC algorithm. One of the contributions of this paper is to show how exact sampling can be done in a flexible and practical way. We describe a MCMC sampler solving this problem in Section 4.

In the following, we parametrize the matrix Langevin by  $(G, \boldsymbol{\kappa}, H)$ , the terms of the SVD of the parameter  $F$ . We place independent priors on these three quantities. Recalling that  $F$  and  $H$  are points on the Stiefel manifolds  $V_{p,d}$  and  $V_{p,p}$  respectively, we place matrix Langevin priors on these as well. We place independent priors on the positive diagonal elements of  $\boldsymbol{\kappa}$  (we write  $\kappa_i$  for element  $(i, i)$  of  $\boldsymbol{\kappa}$ ). Let  $F_0$  parametrize the prior on  $H$ . When this is the all-zero matrix, we have a uniform prior on  $H$ , though more informative priors may also be useful. In particular, it is sometimes desirable to restrict  $F$  to be orthogonal; this amounts to restricting  $H$  to be the identity matrix. Let  $F_1$  parametrize the matrix Langevin prior on  $G$ . The overall generative process is then:

$$\kappa_j \sim \text{Gamma}(a_0, b_0) \quad \text{for } j = 1, \dots, p, \tag{3}$$

$$H \sim \text{P}_{\text{ML}}(H|F_0), \tag{4}$$

$$G \sim \text{P}_{\text{ML}}(G|F_1), \tag{5}$$

$$X_i \sim \text{P}_{\text{ML}}(X_i|G\boldsymbol{\kappa}H^T) \quad \text{for } i = 1, \dots, n. \tag{6}$$

### 3.2 Simulating from the prior

To set the stage for posterior computation, we begin by discussing how to draw a sample from the matrix Langevin distribution. For parameterizations other than the uniform distribution (i.e. for  $\boldsymbol{\kappa} > 0$ ), even this is non-trivial. For simplicity, we assume  $F$  is orthonormal (i.e. that  $H$  equals the identity matrix,  $I_p$ ); in the general case, we simply rotate the resulting draw by  $H$  (since if  $X \sim \text{P}_{\text{ML}}(\cdot|F)$ , then  $XH \sim \text{P}_{\text{ML}}(\cdot|FH^T)$ ). Chikuse (2003b) suggested a simple rejection sampling scheme based on the envelope:

$$\text{etr}(\boldsymbol{\kappa}G^T X) \leq \prod_{i=1}^p \exp(\kappa_i) \tag{7}$$

where the right-hand side is the mode of  $\text{P}_{\text{ML}}(X|G, \boldsymbol{\kappa})$  at  $X = G$ . In this scheme, one proposes values uniformly on  $V_{p,d}$ , accepting a draw  $X$  with probability  $\exp(\boldsymbol{\kappa}G^T X) / \left( \prod_{i=1}^d \exp(\kappa_i) \right)$ . However, this bound is very loose, making this scheme very inefficient. A rejection sampling scheme with a significantly higher acceptance rate was provided in Hoff (2009b). Rather than drawing proposals uniformly on  $V_{p,d}$ , this used the parameters  $G$  and  $\boldsymbol{\kappa}$  to construct a proposal distribution that we outline in Algorithm 1. At a high level, the algorithm sequentially proposes vectors from the vector-valued von Mises Fisher distribution (i.e. the matrix Langevin on the unit sphere), something that is straightforward to do (Wood, 1994). The mean of the  $r$ th vector is the  $r$ th column of  $G$  (call this  $G_{[:,r]}$ ) projected onto the nullspace of the earlier vectors (call this  $N_r$ ). Having sampled this vector on the sphere, it is projected back onto the nullspace  $N_r$  and normalized (giving a unit vector orthogonal to the earlier  $r - 1$  vectors). We describe the algorithm below, for more details, see Hoff (2009b).

---

**Algorithm 1** Proposal distribution  $P_{\text{seq}}(\cdot|F)$  for matrix Langevin distribution (Hoff, 2009b)

---

**Input:** The parameters  $F = G\boldsymbol{\kappa}$  (write  $G_{[:,i]}$  for column  $i$  of  $G$ )

**Output:** An output  $X \in V_{p,d}$  (write  $X_{[:,i]}$  for column  $i$  of  $X$ )

---

1: Sample  $X_{[:,1]} \sim P_{\text{ML}}(\cdot|\boldsymbol{\kappa}_1 G_{[:,1]})$ .

2: For  $r \in \{2, \dots, p\}$

(a) Construct  $N_r$ , an orthogonal basis for the nullspace of  $\{X_{[:,1]}, \dots, X_{[:,r-1]}\}$ .

(b) Sample  $z \sim P_{\text{ML}}(\cdot|\boldsymbol{\kappa}_r N_r^T G_{[:,r]})$ .

(c) Set  $X_{[:,r]} = z^T N_r / \|z^T N_r\|$ .

---

It can be seen that  $X$  has density on the Stiefel manifold given by:

$$P_{\text{seq}}(X|G, \boldsymbol{\kappa}) = \left\{ \prod_{r=1}^p \frac{\|\boldsymbol{\kappa}_r N_r^T G_{[:,r]}/2\|^{(d-r-1)/2}}{\Gamma(\frac{d-r+1}{2}) I_{(d-r-1)/2}(\|\boldsymbol{\kappa}_r N_r^T G_{[:,r]}\|)} \right\} \text{etr}(\boldsymbol{\kappa} G^T X) \quad (8)$$

$$:= \text{etr}(\boldsymbol{\kappa} G^T X) / D(X, \boldsymbol{\kappa}, G) \quad (9)$$

Here,  $I_k(\cdot)$  is the modified Bessel function of the first kind. Since  $I_k(x)/x^k$  is an increasing function of  $x$ , and  $\|\boldsymbol{\kappa}_r N_r^T G_{[:,r]}\| \leq \|G_{[:,r]}\| = 1$ , we have the following bound:

$$D(X, \boldsymbol{\kappa}, G) \leq \prod_{r=1}^p \frac{\Gamma(\frac{d-r+1}{2}) I_{(d-r-1)/2}(\|\boldsymbol{\kappa}_r\|)}{\|\boldsymbol{\kappa}_r/2\|^{(d-r-1)/2}} := D(\boldsymbol{\kappa}) \quad (10)$$

This bound implies that  $\text{etr}(\boldsymbol{\kappa} G^T X) \leq D(\boldsymbol{\kappa}) P_{\text{seq}}(X|G, \boldsymbol{\kappa})$ , and is much tighter than equation (7). Hoff (2009b) uses this to construct the following rejection sampler: draw a sample  $X$  from  $P_{\text{seq}}(\cdot)$ , and accept it with probability  $D(X, \boldsymbol{\kappa}, G)/D(\boldsymbol{\kappa})$ . The set of accepted proposals forms a draw from  $P_{\text{ML}}(\cdot|G, \boldsymbol{\kappa})$ , and to obtain samples from  $P_{\text{ML}}(\cdot|G, \boldsymbol{\kappa}, H)$ , simply post multiply these by  $H$ .

## 4 Posterior sampling

We now return to the problem of posterior inference. With independent priors  $P(G), P(H)$  and  $P(\boldsymbol{\kappa})$  on the parameters  $G, H$ , and  $\boldsymbol{\kappa}$ , and given a set of  $n$  observations  $\{X_i\}$ , we wish to calculate the posterior  $P(G, H, \boldsymbol{\kappa}|\{X_i\})$ . Writing  $S = \sum_{i=1}^n X_i$ , we have:

$$P(G, \boldsymbol{\kappa}, H|\{X_i\}) \propto \frac{\text{etr}(H\boldsymbol{\kappa}G^T S)P(H)P(G)P(\boldsymbol{\kappa})}{Z(\boldsymbol{\kappa})^n}. \quad (11)$$

At a high level, our approach is a Gibbs sampler that sequentially updates  $H, G$  and  $\boldsymbol{\kappa}$ . As described below, the first two steps are straightforward, while the term  $Z(\boldsymbol{\kappa})$  causes complications with the third.

## 4.1 Updating $G$ and $H$ :

The posterior distribution of  $H$  is given by

$$P(H|\{X_i\}, \boldsymbol{\kappa}, G) = P(H|S, \boldsymbol{\kappa}, G) \propto \text{etr}(H\boldsymbol{\kappa}G^T S)P(H). \quad (12)$$

With a matrix Langevin prior on  $H$ ,  $P(H) \propto \text{etr}(H^T F_0)$ , and

$$P(H|\{X_i\}, \boldsymbol{\kappa}, G) \propto \text{etr}((S^T G\boldsymbol{\kappa} + F_0)^T H). \quad (13)$$

This is just a matrix Langevin distribution on the space of rotation matrices, and one can sample from this following section 3.2. For simplicity, from here onwards, we will rotate the observations by  $H$ , allowing us to ignore this term. Thus, redefining  $S$  as  $SH$ , the conditional posterior of  $G$  is given by:

$$P(G|\{X_i\}, \boldsymbol{\kappa}) \propto \text{etr}((S\boldsymbol{\kappa} + F_1)^T G). \quad (14)$$

Again, this is a matrix Langevin distribution that is easy to sample from.

## 4.2 Updating $\boldsymbol{\kappa}$ :

The dependence of the normalization constant on  $\boldsymbol{\kappa}$  makes inference over this parameter trickier. A naïve Metropolis-Hastings (MH) chain that proceeds by proposing a new value  $\boldsymbol{\kappa}^*$  from some density  $q(\boldsymbol{\kappa}^*|\boldsymbol{\kappa})$  has acceptance probability

$$p_{acc} = \frac{\text{etr}(\boldsymbol{\kappa}^*G^T S)P(\boldsymbol{\kappa}^*)q(\boldsymbol{\kappa}|\boldsymbol{\kappa}^*)Z(\boldsymbol{\kappa})^n}{\text{etr}(\boldsymbol{\kappa}G^T S)P(\boldsymbol{\kappa})q(\boldsymbol{\kappa}^*|\boldsymbol{\kappa})Z(\boldsymbol{\kappa}^*)^n}. \quad (15)$$

This itself is intractable (since it involves evaluating  $Z(\boldsymbol{\kappa})$  and  $Z(\boldsymbol{\kappa}^*)$ ), explaining why full Bayesian inference for the matrix Langevin distribution is called doubly intractable.

Our ability to draw perfect samples from the prior means that it is possible to use ideas from the MCMC literature on doubly intractable distributions to deal with this. We start with the exchange sampler of Murray et al. (2006), a standard MCMC algorithm for doubly intractable distributions. While this is an elegant and widely applicable algorithm, it is usually not very efficient without fairly involved annealing schemes. We thus propose an alternate algorithm that exploits the construction of Algorithm 1, allowing significantly greater flexibility and efficiency. Our algorithm is applicable to a wider class of models than the matrix Langevin distribution, and while we leave this for future work, we outline a few directions later.

## 4.3 The exchange sampler

The exchange sampler was proposed by Murray et al. (2006), simplifying an idea by Moller et al. (2006). Applied to the matrix Langevin distribution, the overall algorithm is given in Algorithm 2, and amounts to the following: given the current state  $(G, \boldsymbol{\kappa})$ , propose a

new parameter  $\boldsymbol{\kappa}^*$  according to some proposal distribution  $q(\boldsymbol{\kappa}^*|\boldsymbol{\kappa})$ . Additionally, draw  $n$  auxiliary observations  $\{X_i^*\}$  from the matrix Langevin with parameters  $(G, \boldsymbol{\kappa}^*)$ , and accept  $\boldsymbol{\kappa}^*$  with probability

$$p_{acc} = \frac{P(\boldsymbol{\kappa}^*)q(\boldsymbol{\kappa}|\boldsymbol{\kappa}^*)}{P(\boldsymbol{\kappa})q(\boldsymbol{\kappa}^*|\boldsymbol{\kappa})} \text{etr} \left( (\boldsymbol{\kappa}^* - \boldsymbol{\kappa})G^T \sum_i (X_i - X_i^*) \right). \quad (16)$$

Effectively, having proposed a new parameter and a new dataset, the exchange algorithm attempts to swap the association between parameters and datasets. It is perhaps easiest to understand this algorithm in light of ideas from Andrieu and Roberts (2009). Imagine we have a positive and unbiased (but noisy) estimate  $1/\hat{Z}_n(\boldsymbol{\kappa})$  of the intractable term  $1/Z(\boldsymbol{\kappa})^n$ . Write this as

$$1/\hat{Z}_n(\boldsymbol{\kappa}) = \gamma/Z(\boldsymbol{\kappa})^n \quad \text{with } \gamma \sim P_\gamma(\cdot|n, \boldsymbol{\kappa}), \gamma \geq 0, \text{ and } E_{P_\gamma(\cdot|n, \boldsymbol{\kappa})}[\gamma] = 1. \quad (17)$$

We use this estimate (rather than the intractable  $Z$ ) in computing the MH acceptance ratio of equation (15). Replacing  $Z^n$  with  $\hat{Z}_n$  in equation (15), we see that the Markov transition operator has the stationary distribution  $P(\boldsymbol{\kappa}, \gamma)$  given by:

$$P(\boldsymbol{\kappa}, \gamma) \propto \gamma P(\gamma|n, \boldsymbol{\kappa}) P(\boldsymbol{\kappa}) \frac{\text{etr}(\boldsymbol{\kappa}G^T S)}{Z(\boldsymbol{\kappa})^n}. \quad (18)$$

From the positivity of  $\gamma$ , this is a valid probability distribution, and since  $\gamma$  has expectation 1, this has the desired marginal over  $\boldsymbol{\kappa}$ . The unbiased estimate that Murray et al. (2006) uses is  $\hat{Z}_n = 1/\text{etr}(\boldsymbol{\kappa}G^T \sum_{i=1}^n X_i^*)$ , for  $n$  new variables  $\{X_i^*\}$  drawn i.i.d. from the matrix Langevin distribution. We outline the algorithm below.

---

**Algorithm 2** Exchange sampler for  $\boldsymbol{\kappa}$  (Murray et al., 2006)

---

**Input:** A set of  $n$  observations  $X_i$ ,  
The parameters  $G$  and  $\boldsymbol{\kappa}$

**Output:** A new parameter  $\boldsymbol{\kappa}^*$

---

- 1: Draw  $\boldsymbol{\kappa}^* \sim q(\cdot|\boldsymbol{\kappa})$ .
- 2: Draw  $X_i^* \sim P_{ML}(\boldsymbol{\kappa}^*)$  for  $i \in \{1, \dots, n\}$ .
- 3: Accept this proposal with probability

$$p_{acc} = \frac{P(\boldsymbol{\kappa}^*)q(\boldsymbol{\kappa}|\boldsymbol{\kappa}^*)}{P(\boldsymbol{\kappa})q(\boldsymbol{\kappa}^*|\boldsymbol{\kappa})} \text{etr} \left( (\boldsymbol{\kappa}^* - \boldsymbol{\kappa})G^T \left( \sum_i (X_i - X_i^*)^T \right) \right) \quad (19)$$


---

## 4.4 Sampling by introducing rejected proposals of the rejection sampler

While the exchange algorithm solves the problem of computing the acceptance probability of a proposed  $\boldsymbol{\kappa}^*$ , there still remains the problem of making *good* proposals. For the latter, one

either has to make very local updates to  $\boldsymbol{\kappa}$ , or resort to complicated annealing schemes to obtain better estimates of  $\hat{Z}$ . Adams et al. (2009) report other problems with the exchange sampler.

Instead, it would be advantageous to harness the computational cost of generating each auxiliary variable  $X_i^*$  towards proposing a good  $\boldsymbol{\kappa}^*$ . Under the rejection sampling scheme of Hoff (2009b), any observation on the Stiefel manifold is preceded by a set (possibly of size zero) of rejected proposals. A simple idea is to first conditionally sample this set of rejected proposals, and *then* propose a new  $\boldsymbol{\kappa}^*$  given these auxiliary variables. We show that the rejected events can be sampled efficiently and easily, and that since  $P_{\text{seq}}$  does not involve any intractable terms, standard MCMC techniques can be applied to make efficient proposals for  $\boldsymbol{\kappa}$ . While the exchange sampler is applicable to any model from which one can draw perfect samples, our approach can offer advantages when rejection sampling is used (see Adams et al. (2009), and Beskos and Roberts (2005) for other such models).

Let  $\mathcal{Y} = \{Y_1, \dots, Y_r\}$  be the sequence of  $r \geq 0$  rejected proposals preceding an observation. From section 3.2, the probability of the entire set is

$$P(\mathcal{Y}, X) = \frac{\text{etr}(\boldsymbol{\kappa}G^T (X + \sum_{i=1}^{|\mathcal{Y}|} Y_i))}{D(\boldsymbol{\kappa})^{1+|\mathcal{Y}|}} \prod_{i=1}^{|\mathcal{Y}|} \frac{(D(\boldsymbol{\kappa}) - D(Y_i, G, \boldsymbol{\kappa}))}{D(Y_i, G, \boldsymbol{\kappa})}. \quad (20)$$

All terms in the expression above can be evaluated easily, and by construction,  $X$  is marginally distributed as the matrix Langevin: introducing the auxiliary set  $\mathcal{Y}$  has eliminated the intractable normalization constant  $Z(\boldsymbol{\kappa})$ . Thus, given an observation  $X$ , inference over  $\boldsymbol{\kappa}$  would be straightforward once we instantiate  $\mathcal{Y}$  from  $P(\mathcal{Y}|X)$  (and given a set of observations  $\{X_1, \dots, X_n\}$ , we instantiate a set  $\mathcal{Y}_i$  for each observation  $X_i$ ).

Below, we show that simulating  $\mathcal{Y}|X$  involves the following two steps: draw points  $Y_i$  i.i.d. from the proposal distribution until an acceptance (call the accepted point  $\hat{X}$ ). Then, discard  $\hat{X}$ , and treat the set of rejected events as  $\mathcal{Y}$ . While it is possible to show this is correct by writing down the density  $P(\mathcal{Y}|X)$ , this is complicated by the fact that  $\mathcal{Y}$  take values over a union of a product of Stiefel manifolds, one for each possible length  $|\mathcal{Y}|$ . Instead, we provide a clearer proof of the correctness of our sampler below.

**Proposition 4.1.** *The set of points  $\mathcal{Y}$  preceding an observation  $X$  is independent of  $X$ . We can therefore assign  $\mathcal{Y}$  a set of rejected variables associated with some other sample,  $\hat{X}$ .*

*Proof.* For parameters  $(\boldsymbol{\kappa}, G)$ , the probability of an observation  $X$  is

$$P(X|\boldsymbol{\kappa}, G) = \frac{\text{etr}(\boldsymbol{\kappa}G^T X)}{Z(\boldsymbol{\kappa})}. \quad (21)$$

Independently introducing the set  $(\mathcal{Y}, \hat{X})$ , the joint probability is now

$$P(X, \mathcal{Y}, \hat{X}|G, \boldsymbol{\kappa}) = \frac{\text{etr}(\boldsymbol{\kappa}G^T X)}{Z(\boldsymbol{\kappa})} \left( \prod_{i=1}^{|\mathcal{Y}|} \frac{\text{etr}(\boldsymbol{\kappa}G^T Y_i)}{D(Y_i, G, \boldsymbol{\kappa})} \left( 1 - \frac{D(Y_i, G, \boldsymbol{\kappa})}{D(\boldsymbol{\kappa})} \right) \right) \frac{\text{etr}(\boldsymbol{\kappa}G^T \hat{X})}{D(\boldsymbol{\kappa})}.$$



Now, swapping  $X$  and  $\hat{X}$ , we see that  $P(\hat{X}, \mathcal{Y}, X|G, \boldsymbol{\kappa}) = P(X, \mathcal{Y}, \hat{X}|G, \boldsymbol{\kappa})$ . Marginalizing out  $\hat{X}$ , we have

$$P(\mathcal{Y}, X) = \prod_{i=1}^{|\mathcal{Y}|} \left( 1 - \frac{\text{etr}(\boldsymbol{\kappa}G^T Y_i)}{D(Y_i, G, \boldsymbol{\kappa})} \right) \frac{\text{etr}(\boldsymbol{\kappa}G^T X)}{D(X, G, \boldsymbol{\kappa})}. \quad (22)$$

This is the desired joint distribution, proving our sampling scheme is correct.  $\square$

The exchange sampler, which involves drawing a perfect sample from the model, has to implicitly generate a new set of auxiliary thinned variables for every proposal  $\boldsymbol{\kappa}^*$ . By contrast, we explicitly instantiate the thinned variables first, and then propose a new parameter  $\boldsymbol{\kappa}^*$ . This proposal is accepted or rejected according to the usual Metropolis-Hastings ratio, with equation (22) giving the likelihood term. Keeping the auxiliary variables, we can successively make a number of proposals for  $\boldsymbol{\kappa}^*$  without having to generate new auxiliary observations, offering computational savings. Additionally, we can exploit the tractability of the joint distribution, using, for example, gradient information and Hamiltonian Monte Carlo (Neal, 2010) to make significantly more efficient proposals than the random walk MH sampler. We demonstrate this below.

Given  $n$  observations  $X_1, \dots, X_n$  with latent variable sets  $\mathcal{Y}_1, \dots, \mathcal{Y}_n$ , let  $N = n + \sum_{i=1}^n |\mathcal{Y}_i|$ , and  $S = \sum_{i=1}^n (X_i + \sum_{j=1}^{|\mathcal{Y}_i|} Y_{i,j})$ . The log joint probability is

$$\begin{aligned} L \equiv \log(P(\{X_i, \mathcal{Y}_i\})) &= \text{trace}(G^T \boldsymbol{\kappa} S) + \sum_{i=1}^n \sum_{j=1}^{|\mathcal{Y}_i|} (\log(D(\boldsymbol{\kappa}) - D(Y_{i,j}, \boldsymbol{\kappa})) \\ &\quad - \log(D(Y_{i,j}, \boldsymbol{\kappa}))) - N \log(D(\boldsymbol{\kappa})). \end{aligned} \quad (23)$$

Noting that  $D(Y, \boldsymbol{\kappa}) = \left\{ C \prod_{r=1}^p \frac{I_{(d-r-1)/2}(\|\boldsymbol{\kappa}_r N_r^T G_r\|)}{\|\boldsymbol{\kappa}_r N_r^T G_r\|^{(d-r-1)/2}} \right\} := C \tilde{D}(Y, \boldsymbol{\kappa})$ , we can show (see Appendix A) that

$$\begin{aligned} \frac{dL}{d\boldsymbol{\kappa}_k} &= G_{[k]}^T S_{[k]} + \sum_{i=1}^n \sum_{j=1}^{|\mathcal{Y}_i|} \left( \frac{\frac{I_{(d-k+1)/2}(\boldsymbol{\kappa}_k) - N_k^T G_k \frac{I_{(d-k+1)/2}(\boldsymbol{\kappa}_k N_k^T G_k)}{I_{(d-k-1)/2}(\boldsymbol{\kappa}_k N_k^T G_k)}}{(1 - \frac{\tilde{D}(Y_{i,j}, \boldsymbol{\kappa})}{\tilde{D}(\boldsymbol{\kappa})}})}{1 - \frac{\tilde{D}(Y_{i,j}, \boldsymbol{\kappa})}{\tilde{D}(\boldsymbol{\kappa})}} \right) \\ &\quad - N \frac{I_{(d-k+1)/2}(\boldsymbol{\kappa}_k)}{I_{(d-k-1)/2}(\boldsymbol{\kappa}_k)}. \end{aligned} \quad (24)$$

We use this gradient information to construct a Hamiltonian system, and following Neal (2010), construct an MCMC algorithm that explores values of  $\boldsymbol{\kappa}$  more efficiently than the random walk Metropolis-Hastings algorithm. The resulting Hamiltonian Monte Carlo (HMC) sampler is a fairly standard MCMC algorithm, and we refer the reader to Neal (2010) for details. For our purposes, it suffices to note that a proposal of the HMC sampler involves taking a number  $L$  of ‘leapfrog’ steps of size  $\epsilon$  along the gradient, and then accepting the resulting state with probability proportional to the product of equation (22), and a simple Gaussian term (corresponding to a ‘momentum’ term). The acceptance probability depends

on how accurately the  $\epsilon$ -discretization approximates the continuous dynamics of the system, and by choosing a small  $\epsilon$  and a large  $L$ , one can make global moves with high acceptance probability. On the other hand, a large  $L$  comes at the cost of a large number of gradient evaluations. We study this trade-off in Section 5.

## 4.5 Related work

Most closely related to our latent variable sampler is a sampler proposed in Adams et al. (2009). While their problem was different, it too involved inferences on the parameters governing the output of a rejection sampler. Like us, they proceeded by augmenting the MCMC state space to include the rejected samples (call them  $\mathcal{Y}$ ), noting that this simplifies the posterior over the parameters of interest. However, rather than generating independent realizations of  $\mathcal{Y}$  when needed (Proposition 4.4 shows this is easy), Adams et al. (2009) proposed a set of Markov transition operators to perturb the current configuration of  $\mathcal{Y}$ , while maintaining the correct stationary distribution. In particular, with prespecified probabilities, they proposed adding a new variable to  $\mathcal{Y}$ , deleting a random variable from  $\mathcal{Y}$  and perturbing the value of an existing elements in  $\mathcal{Y}$ . These local updates to  $\mathcal{Y}$  can slow down Markov chain mixing, require the user to specify a number of parameters, and also involves calculating Metropolis-Hastings acceptance probabilities for each local step. By contrast, Proposition 4.4 describes a simple and efficient scheme to instantiate these rejected variables.

Additionally, in our problem, adding a persistent set of variables  $\mathcal{Y}$  to the state space of the Markov chain leads to complications: note that  $\mathcal{Y}$  depends on the parameters  $G$  and  $H$ , so that conditioned on  $\mathcal{Y}$ , the posterior distributions over  $G$  and  $H$  are no longer conjugate. Thus, with  $\mathcal{Y}$  instantiated, the sampler of Adams et al. (2009) would require complicated alternatives to the simple steps in Section 4.1 to explore the high-dimensional spaces these variables live in. Instead, Proposition 4.4 allows our sampler to discard the set  $\mathcal{Y}$ , reintroducing it only when we need to update the doubly intractable parameter  $\boldsymbol{\kappa}$ .

Another auxiliary variable approach was proposed recently in Walker (2011); however this requires bounding  $P_{\text{ML}}(X|\boldsymbol{\kappa}, G)$  uniformly over all three variables. Even if we allow this (by limiting the components  $\kappa_i$  to a compact sets), the algorithm will scale with the volume of the Stiefel manifold, and quickly becomes unmanageable.

## 4.6 Approximate inference

Both samplers described previously have the disadvantage of scaling with the number of observations  $n$ . In settings where  $n$  is large, they can be very computationally intensive, and it is worth considering approximations to the posterior over  $\boldsymbol{\kappa}$ . An asymptotic approximation for large values of  $(\kappa_1, \dots, \kappa_n)$  is provided in Khatri and Mardia (1977):

$$Z(\boldsymbol{\kappa}) = {}_0F_1\left(\frac{1}{2}d, \frac{1}{4}\boldsymbol{\kappa}^T\boldsymbol{\kappa}\right) \simeq \left\{2^{-\frac{1}{4}p(p+5)+\frac{1}{2}pd}\pi^{-\frac{1}{2}p}\right\} \prod_{j=1}^p \Gamma\left(\frac{d-j+1}{2}\right)$$

$$\text{etr}(\boldsymbol{\kappa}) \left[ \left\{ \prod_{j=2}^p \prod_{i=1}^{j-1} (\kappa_i + \kappa_j)^{\frac{1}{2}} \right\} \prod_{i=1}^p \kappa_i^{\frac{1}{2}(d-p)} \right]^{-1}. \quad (25)$$

An expansion, similar in spirit, but for the matrix Bingham distribution was used by Hoff (2009a). Plugging this approximation in the acceptance probability of a Metropolis-Hastings algorithm allows the construction of a straightforward MCMC algorithm; similarly this can easily be extended to incorporate gradient information via Hamiltonian dynamics. A drawback with such approximate MCMC schemes is that they involve the ratio of two approximations, and therefore can have very unpredictable performance. In the next section, we study the behaviour of this approximation along with the performance of exact samplers.

## 5 Experiments

In the experiments below, we study the performance of the different MCMC samplers described above. We implemented all algorithms in R, building on code from the `rstiefel` package (Hoff, 2013). All simulations were run on an Intel Core 2 Duo 3 Ghz CPU.

### 5.1 Comparison of exact MCMC samplers

In our first experiment, we compare the performance of the different exact samplers for the matrix Langevin distribution. To measure how efficiently these explore parameter values, we estimate the effective sample sizes (ESSs) produced per unit time. The ESS corrects for correlation between successive Markov chain samples by trying to estimate the number of independent samples produced; for this we used the `rcoda` package of Plummer et al. (2006). We consider the vector cardiogram dataset (Downs et al., 1971b), consisting of 98 observations on  $V_{3,2}$ . This dataset is standard in the Stiefel manifold modeling literature, with each observation giving the orientation of the so-called QRS loop in three dimensions. We describe the dataset and the prior specification more carefully in Section 5.3.

The left plot in Figure 1 considers two Metropolis-Hastings samplers, the exchange sampler and our latent variable sampler. Both samplers perform a random walk in the  $\boldsymbol{\kappa}$ -space, with the steps drawn for a normal distribution whose variance increases along the horizontal axis. The vertical axis shows the median ESS per second for the components of  $\boldsymbol{\kappa}$ . The figure shows that both samplers' performance peaks when the proposals have a variance between 1 and 1.5, with the exchange sampler performing slightly better. However, as pointed out, the real advantage of our sampler is that introducing the latent variables results in a joint distribution without any intractable terms, allowing the use of more sophisticated MCMC algorithms. The plot to the right studies the Hamiltonian Monte Carlo sampler described at the end of Section 4.4. We study this algorithm by varying the size of the leapfrog steps along the horizontal axis, with the different curves corresponding to different numbers of leapfrog steps<sup>1</sup>. We see that this performs an order of magnitude better than either of the

---

<sup>1</sup>We fix the mass parameter to the identity matrix as is typical.

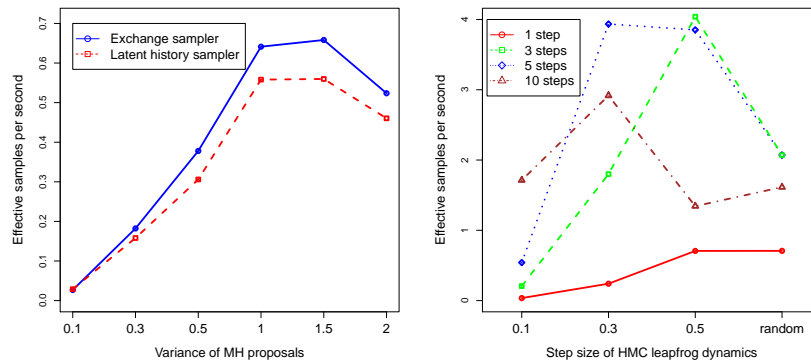


Figure 1: Effective sample size per second for (left) MH, and (right) HMC samplers

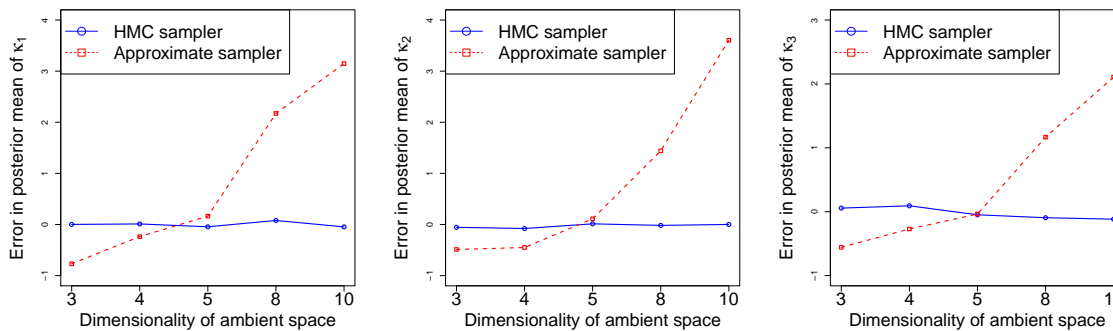


Figure 2: Errors in the posterior mean

previous algorithms, with performance peaking with 3 to 5 steps of size 0.3 to 0.5, fairly typical values for this algorithm. This shows the benefit afforded by exploiting gradient information in exploring the parameter space.

## 5.2 Study of the approximate MCMC sampler

On the vectorcardiogram dataset, the approximate MCMC sampler based on the asymptotic expansion of equation (25) is about forty times faster than the exact samplers. For larger datasets, this difference will be even greater, and the real question is how accurate the approximation is. We study how this approximation behaves for different values of  $\kappa$  and for different dimensionalities of the ambient space. In particular, we consider the Stiefel manifold  $V_{d,3}$ , with the three diagonal elements of  $\kappa$  set to 1, 5 and 10. With this setting of  $\kappa$ , and a random  $G$ , we generate datasets with 50 observations with  $d$  taking values 3, 4, 5, 8, and 10. In each case, we estimate the posterior mean of  $\kappa$  by running the exchange sampler, and treat this as the truth. We compare this with posterior means returned by the HMC sampler and the approximate sampler. Figure 2 shows these results, with the three

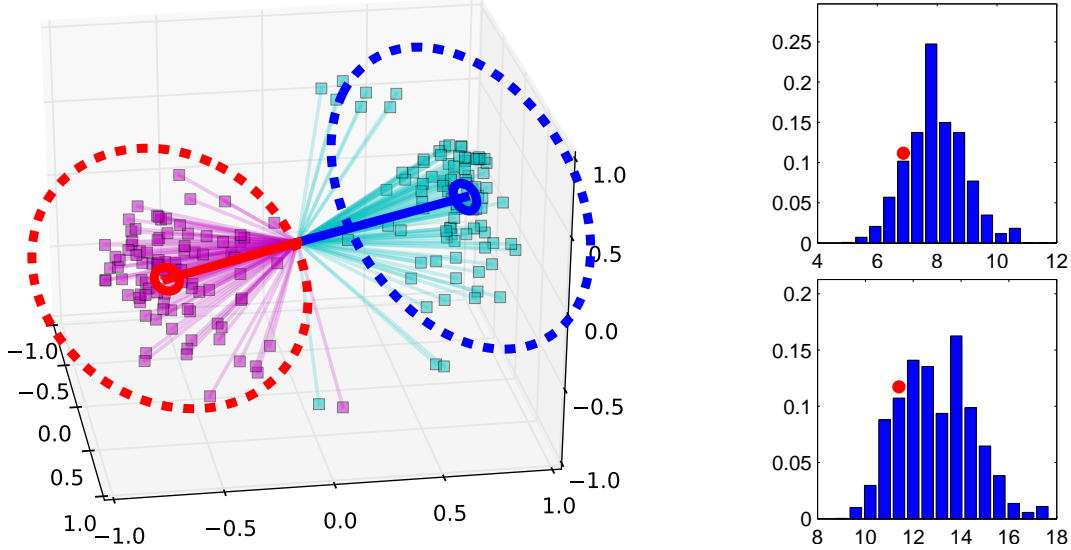


Figure 3: (Left) Vector cardiogram dataset with inference summaries. The bold lines are ML estimates of the components of  $G$ , while the small circles contain 90% of the posterior samples of  $G$ . The large, dashed circles account for  $\kappa$  as well, and contain 90% of the predictive probability mass for new observations. (Right) Posterior distributions over  $\kappa_1$  and  $\kappa_2$ . The red circles are ML estimates.

subplots corresponding to the three components of  $\kappa$ , and with the ambient dimensionality  $d$  increasing along the horizontal axis.

As one would expect, the two exact samplers agree with each other, and the HMC sampler has almost no ‘error’. On the other hand, the behaviour of the approximate sampler is more complicated. For values of  $d$  around 5, its estimated posterior mean is close to that of the exact samplers. Smaller values lead to an approximate posterior mean that underestimates the actual posterior mean, while in higher dimensions, the opposite occurs. Recalling that  $\kappa$  controls the concentration of the matrix Langevin distribution about its mode, this implies that in high dimensions, the approximate sampler will underestimate uncertainty in the distribution of future observations.

### 5.3 Vectorcardiogram dataset

The vectorcardiogram (VCG) is a loop traced by the cardiac vector during a cycle of the heart beat. The two directions of orientation of this loop in three-dimensional space form a point on the Stiefel manifold. The VCG dataset from Downs et al. (1971a) is a collection of 98 such recordings, and is displayed in the left subplot of Figure 3. Here, we represent each observation with a pair of orthonormal vectors, with the set of cyan lines forming the first component, and the magenta lines the second (we explain the rest of the figure later). Clearly, the empirical distribution of these observations possesses a single mode, and the matrix Langevin distribution is an appropriate model for these observations.

Table 1: Log predictive-probability of 20 random held out observations, averaged over 5 runs.

	MLE	Bayesian inference
Log predictive-probability	$68.78 \pm 9.96$	$78.72 \pm 8.26$

We place independent uninformative exponential priors with mean 10 (and variance 100) on the scale parameter  $\boldsymbol{\kappa}$ , and a uniform prior on the location parameter  $G$ . As before, we restrict  $H$  to be the identity matrix. Inferences were carried out using the HMC sampler to produce 10,000 samples, with a burn-in period of 1,000. For the leapfrog dynamics, we set a step size of 0.3, with the number of steps equal to 5.

For comparison, we use the maximum likelihood estimates of the parameters  $\boldsymbol{\kappa}$  and  $G$ . Obtaining the MLE of  $G$  is straightforward (Khatri and Mardia, 1977); and for  $\boldsymbol{\kappa}$ , we follow Khatri and Mardia (1977) and use the approximation of equation (25) for  $Z(\boldsymbol{\kappa})$ . Performing a grid search over the interval 0 to 20, we obtain ML estimates of 11.9 and 5.9 for  $\kappa_1$  and  $\kappa_2$ . These are plotted in the right half of Figure 3 as the red circles, with the blue bars showing the Bayesian posteriors over these components. Similarly, the bold straight lines in Figure 3(left) show the MLE estimates of the components of  $G$ , with the small circles corresponding to 90% Bayesian credible regions estimated from the MCMC output. The dashed circles correspond to 90% predictive probability regions for the Bayesian model. To produce these, we generated 50 points on  $V_{3,2}$  for each MCMC sample, with parameters specified by that sample. The dashed circles contain 90% of the generated points across all MCMC samples.

To quantitatively compare the Bayesian posterior with the ML estimate, we ran a 5-fold cross-validation, holding out a random 20 percent of the observations (call this  $X_{test}$ ), and training the models on the remaining data (call this  $X_{train}$ ). Table 1 compares the log probability of the test data under the maximum likelihood estimate,  $P(X_{test}|\hat{\boldsymbol{\kappa}}_{MLE}, \hat{G}_{MLE})$ , with the predictive probability  $P(X_{test}|X_{train}) = \int P(X_{test}|\boldsymbol{\kappa}, G)P(\boldsymbol{\kappa}, G|X_{train})d\boldsymbol{\kappa}dG$ . We approximated the latter integral by a summation over the MCMC samples, and to evaluate the probabilities  $P(X_{test}|\boldsymbol{\kappa}, G)$  for both methods, we approximated  $Z(\boldsymbol{\kappa})$  using equation (25). We see that the log predictive-probability under the Bayesian approach exceeds that of the MLE by about 10, and demonstrates the importance of maintaining uncertainty over the matrix Langevin parameters.

## 6 Nonparametric extensions

In many situations, assuming the observations come from a particular parametric family is restrictive, and raises concerns about model misspecification. Nonparametric alternatives are more flexible and have much wider applicability, and we consider these in this section.

Denote by  $\mathcal{M}$  the space all the densities on  $V_{p,d}$  with respect to the Haar measure  $\lambda$ . Let  $g(X, G, \boldsymbol{\kappa})$  be a parametric kernel on the Stiefel manifold with a ‘location parameter’  $G$  and a vector of concentration parameters  $\boldsymbol{\kappa} = \{\kappa_1, \dots, \kappa_p\}$ . One can place a prior  $\Pi$  on  $\mathcal{M}$  by

modelling the random density  $f$  as

$$f(X) = \int g(X, G, \boldsymbol{\kappa}) P(d\boldsymbol{\kappa}dG), \quad (26)$$

with the mixing measure  $P$  a random probability measure. A popular prior over  $P$  is the Dirichlet process (Ferguson, 1973), parametrized by a base probability measure  $P_0$  on the product space  $\mathbb{R}_+^p \times V_{p,d}$ , and a concentration parameter  $\alpha > 0$ . We denote by  $\Pi_1$  the DP prior on the space of mixing measures, and assume  $P_0$  has full support on  $\mathbb{R}_+^p \times V_{p,d}$ .

The model in (26) is a ‘location-scale’ mixture model, and corresponds to an infinite mixture model where each component has its own location and scale. One can also define the following ‘location’ mixture model given by

$$f(X) = \int g(X, G, \boldsymbol{\kappa}) P(dG)\mu(d\boldsymbol{\kappa}), \quad (27)$$

where  $P$  is given a nonparametric prior like the DP and  $\mu(d\boldsymbol{\kappa})$  is a parametric distribution (like the Gamma or Weibull distribution). In this model, all components are constrained to have the same scale parameters  $\boldsymbol{\kappa}$ .

When  $\Pi_1$  corresponds to a DP prior, one can precisely quantify the mean of the induced density  $\Pi$ . For model (26), the mean prior is given by

$$E(f(X)) = \int g(X, G, \boldsymbol{\kappa}) E(P(d\boldsymbol{\kappa}dG)) = \int g(X, G, \boldsymbol{\kappa}) P_0(d\boldsymbol{\kappa}dG), \quad (28)$$

while for model (27), this is

$$E(f(X)) = \int g(X, G, \boldsymbol{\kappa}) \mu(d\boldsymbol{\kappa}) P_0(dG). \quad (29)$$

The parameter  $\alpha$  controls the concentration of the prior around the mean, and one can place a hyperprior on this as well.

In the following, we set  $g(X, G, \boldsymbol{\kappa})$  to be the matrix Langevin distribution with parameter  $F = G\boldsymbol{\kappa}$ . Thus,

$$g(X, G, \boldsymbol{\kappa}) = \text{etr}(\boldsymbol{\kappa}G^T X) / Z(\boldsymbol{\kappa}) = C(\boldsymbol{\kappa}) \text{etr}(\boldsymbol{\kappa}G^T X), \quad (30)$$

with  $C(\boldsymbol{\kappa}) = 1/Z(\boldsymbol{\kappa}) = 1/{}_0F_1(\frac{1}{2}d, \frac{1}{4}\boldsymbol{\kappa}^T \boldsymbol{\kappa})$ . Note that we have restricted ourselves to the special case where the matrix Langevin parameter  $F$  has orthogonal columns (or equivalently, where  $H = I_p$ ). While it is easy to apply our ideas to the general case, we demonstrate below that even with this restricted kernel, our nonparametric model has properties like large support and consistency.

## 6.1 Posterior consistency

With our choice of parametric kernel, a DP prior on  $\Pi_1$  induces an infinite mixture of matrix Langevin distributions on  $\mathcal{M}$ . Call this distribution  $\Pi$ ; below, we show that this has large

support on  $\mathcal{M}$ , and that the resulting posterior distribution concentrates around any true data generating density in  $\mathcal{M}$ . Our modelling framework and theory builds on Bhattacharya and Dunson (2010, 2012), who developed consistency theorems for density estimation on compact Riemannian manifolds, and considered DP mixtures of kernels appropriate to the manifold under consideration. However, they only considered simple manifolds, and showing that our proposed models have large support and consistency properties requires substantial new theory.

We first introduce some notions of distance and neighborhoods on  $\mathcal{M}$ . A weak neighborhood of  $f_0$  with radius  $\epsilon$  is defined as

$$W_\epsilon(f_0) = \left\{ f : \left| \int z f \lambda(dX) - \int z f_0 \lambda(dX) \right| \leq \epsilon, \text{ for all } z \in C_b(V_{p,d}) \right\}, \quad (31)$$

where  $C_b(V_{p,d})$  is the space of all continuous and bounded functions on  $V_{p,d}$ . The Hellinger distance  $d_H(f, f_0)$  is defined as

$$d_H(f, f_0) = \left( \frac{1}{2} \int (\sqrt{f(X)} - \sqrt{f_0(X)})^2 \lambda(dX) \right)^{1/2}.$$

We let  $U_\epsilon(f_0)$  denote an  $\epsilon$ -Hellinger neighborhood around  $f_0$  with respect to  $d_H$ . The Kullback-Leibler (KL) divergence between  $f_0$  and  $f$  is defined to be

$$d_{KL}(f_0, f) = \int f_0(X) \log \frac{f_0(X)}{f(X)} \lambda(dX), \quad (32)$$

with  $K_\epsilon(f_0)$  denoting an  $\epsilon$ -KL neighborhood of  $f_0$ .

Let  $X_1, \dots, X_n$  be  $n$  observations drawn i.i.d. from some true density  $f_0$  on  $V_{p,d}$ . Under our model, the posterior probability  $\Pi_n$  of some neighborhood  $W_\epsilon(f_0)$  is given by

$$\Pi_n(W_\epsilon(f_0) | X_1, \dots, X_n) = \frac{\int_{W_\epsilon(f_0)} \prod_{i=1}^n f(X_i) \Pi(df)}{\int_{\mathcal{M}} \prod_{i=1}^n f(X_i) \Pi(df)}. \quad (33)$$

The posterior is weakly consistent if for all  $\epsilon > 0$ , the following holds:

$$\Pi_n(W_\epsilon(f_0) | X_1, \dots, X_n) \rightarrow 1 \text{ a.s. } P f_0^\infty \text{ as } n \rightarrow \infty, \quad (34)$$

where  $P f_0^\infty$  represents the true probability measure for  $(X_1, X_2, \dots)$ .

We assume the true density  $f_0$  is continuous with  $F_0$  as its probability distribution. The following theorem is on the weak consistency of the posterior under the mixture prior for both models (26) and (27), the proof of which is included in the appendix.

**Theorem 6.1.** *The posterior  $\Pi_n$  in the DP-mixture of matrix Langevin distributions is weakly consistent.*

We now consider the consistency property of the posterior  $\Pi_n$  with respect to the Hellinger neighborhood  $U_\epsilon(f_0)$ , this is referred as strong consistency.



**Theorem 6.2.** *Let  $\pi_{\boldsymbol{\kappa}}$  be the prior on  $\boldsymbol{\kappa}$ , and let  $\Pi$  be the prior on  $\mathcal{M}$  induced by  $\Pi_1$  and  $\pi_{\boldsymbol{\kappa}}$  via the mixture model (27). Let  $\Pi_1 \sim DP_{\alpha P_0}$  with  $P_0$  a base measure having full support on  $V_{p,d}$ . Assume  $\pi_{\boldsymbol{\kappa}}(\phi^{-1}(n^a, \infty)) \leq \exp(-n\beta)$  for some  $a < 1/((p+2)dp)$  and  $\beta > 0$  with  $\phi(\boldsymbol{\kappa}) = \sqrt{\sum_{i=1}^p (\kappa_i + 1)^2}$ . Then the posterior  $\Pi_n$  is consistent with respect to the Hellinger distance  $d_H$ .*

**Remark 6.1.** *For prior  $\pi_{\boldsymbol{\kappa}}$  on the concentration parameter  $\boldsymbol{\kappa}$ , to satisfy the condition  $\pi_{\boldsymbol{\kappa}}(\phi^{-1}(n^a, \infty)) < \exp(-n\beta)$ , for some  $a < 1/(dp(p+2))$  and  $\beta > 0$  requires fast decay of the tails for  $\pi_{\boldsymbol{\kappa}}$ . One can check that an independent Weibull prior for  $\kappa_i$ ,  $i = 1, \dots, p$  with  $\kappa_i \sim \kappa_i^{(1/a)-1} \exp(-b\kappa_i^{1/a})$  will satisfy the tail condition.*

*Another choice is to allow  $\pi_{\boldsymbol{\kappa}}$  to be sample size dependent as suggested by Bhattacharya and Dunson (2012). In this case, one can choose independent Gamma priors for  $\kappa_i$  with  $\kappa_i \sim \kappa_i^c \exp(-b_n \kappa_i)$  where  $c > 0$  and  $n^{1-a}/b_n \rightarrow 0$  with  $0 < a < 1/(dp(p+2))$ .*

## 6.2 Inference for the nonparametric model

The auxiliary variable representation of equation (22) makes it easy to construct MCMC samplers for the nonparametric model. Here, we limit ourselves to samplers based on the Chinese restaurant process (CRP) representation of the DP (Neal, 2000), though Appendix C discusses alternatives.

The Chinese restaurant process describes the distribution over partitions of observations that results from integrating out the DP-distributed discrete random probability measure  $\Pi$ . A CRP-based sampler updates this partition by reassigning each observation to a cluster conditioned on the rest. The probability of an observation  $(X_i, \mathcal{Y}_i)$  joining a cluster with given parameters is proportional to the likelihood of equation (22) and the number of observations already at that cluster (for an empty cluster, the latter is the concentration parameter  $\alpha$ ). The parameters of each cluster can be updated using the algorithms of Section 4. We provide details in Appendix C, since these are standard for DP mixture models. We also describe an alternate exchange-sampler based approach to updating the partitions in the appendix.

## 7 Experiments

In this section, we apply our nonparametric model to a dataset of near-Earth astronomical objects (comets and asteroids). We implemented the CRP-based sampler of the previous section in R, with cluster parameters updated using the HMC sampler from the parametric case. Inferences were based on 5,000 samples from the MCMC sampler, after a burn-in period of 1,000 samples.

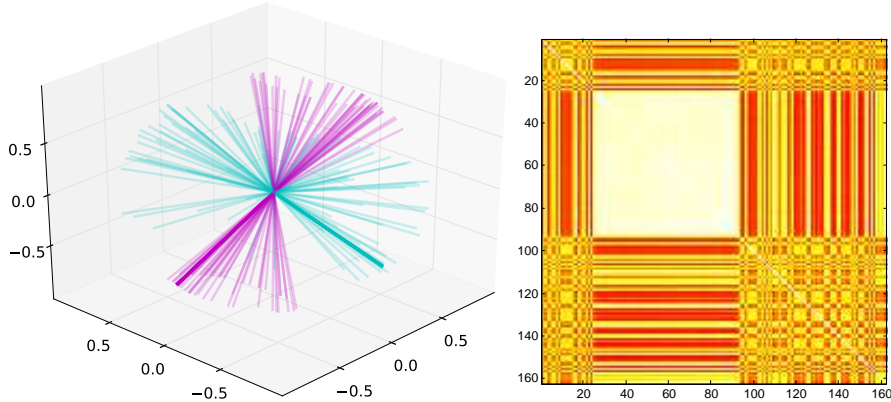


Figure 4: The Near Earth Objects dataset (left), and the adjacency matrix inferred by the DP mixture model (right)

## 7.1 Near Earth Objects dataset

The Near Earth Objects dataset was collected by the Near Earth Object Program of the National Aeronautics and Space Administration<sup>2</sup>, and consists of 162 observations. Each data point lies on the Stiefel manifold  $V_{3,2}$ , and characterizes the orientation of a two-dimensional elliptical orbit in three-dimensional space. The left subplot in Figure 4 shows these data, with each 2-frame represented as two orthonormal unit vectors. The first component (representing the latitude of perihelion) is the set of cyan lines arranged as two horizontal cones. The magenta lines (arranged as two vertical cones) form the second component, the longitude of perihelion.

We model this dataset as a DP mixture of matrix Langevin distributions. We set the DP concentration parameter  $\alpha$  to 1, and for the DP base measure, placed independent probability measures on the matrices  $G$  and  $\kappa$ . For the former, we used a uniform prior (as in Section 3); however we found that an uninformative prior on  $\kappa$  resulted in high posterior probability for a single diffuse cluster with no interesting structure. To discourage this, we sought to penalize small values of  $\kappa_i$ . One way to do this is to use a Gamma prior with a large shape parameter. Another is to use a hard constraint to bound the  $\kappa_i$ 's away from small values. We took the latter approach, placing independent exponential priors restricted to  $[5, \infty)$  on the diagonal elements of  $\kappa$ .

The right plot in Figure 4 shows the adjacency matrix summarizing the posterior distribution over clusterings. An off-diagonal element  $(i, j)$  gives the number of times observations  $i$  and  $j$  were assigned to the same cluster under the posterior. We see a highly coupled set of observations (from around observation 20 to 80 keeping the ordering of the downloaded dataset). This cluster corresponds to a tightly grouped set of observations, visible as a pair of bold lines in the left plot of Figure 4.

To investigate the underlying structure more carefully, we plot in Figure 5 the posterior distribution over the number of clusters. The figure shows this number is peaked at 4,

<sup>2</sup>Downloaded from [http://neo.jpl.nasa.gov/cgi-bin/neo\\_elem](http://neo.jpl.nasa.gov/cgi-bin/neo_elem)

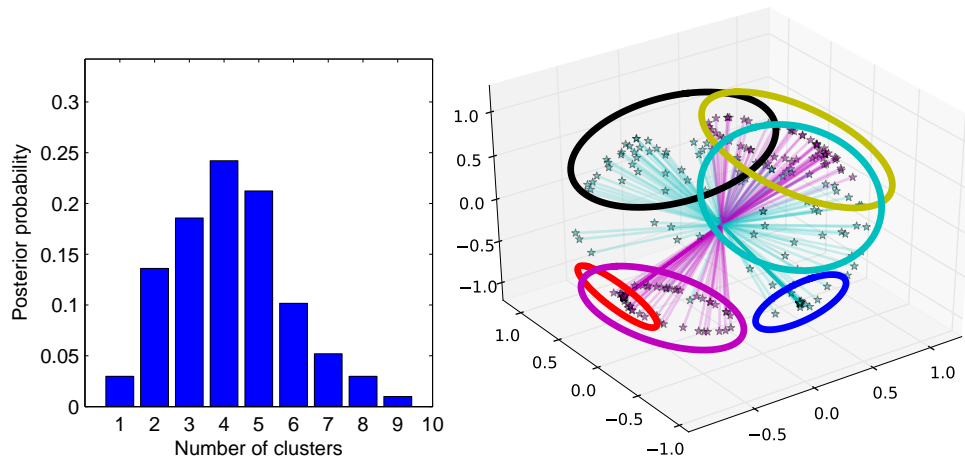


Figure 5: Posterior over the number of clusters for the Near Earth Objects dataset (left), and location and scale parameters of an MCMC sample with three clusters (right). The circles associated with each cluster correspond to 75% predictive probability regions for the associated component.

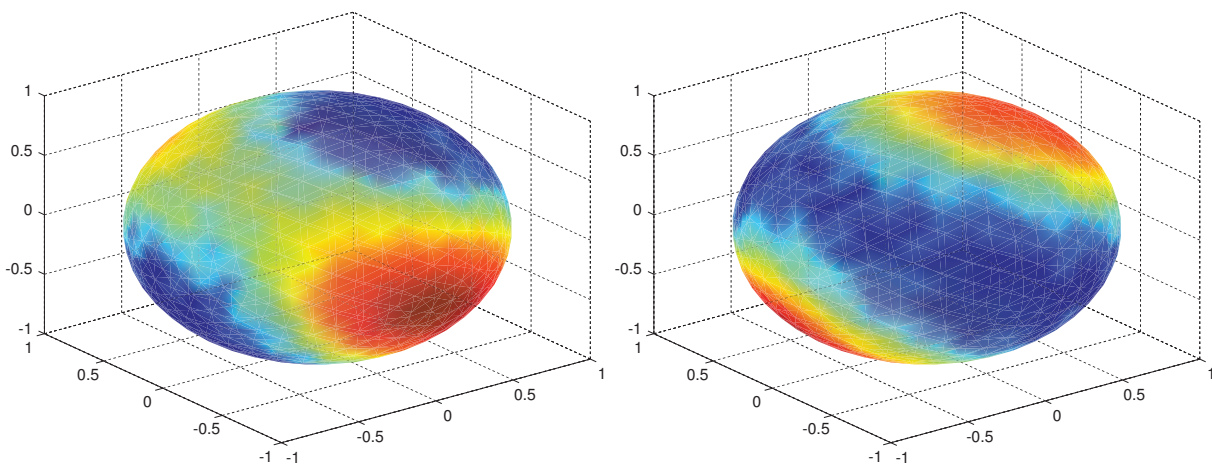


Figure 6: Log predictive probabilities of first and second orthonormal components.

extending up to 9. However, in most instances, most clusters have a small number of observations, with the posterior dominated by 2 or 3 large clusters. A typical two cluster realization is fairly intuitive, with each cluster corresponding to one of the two pairs of cones at right angles, and these clusters were identified quite consistently across all posterior samples. Occasionally, one or both of these might be further split into two smaller clusters, resulting in 3 or 4 clusters. A different example of a three cluster structure is shown in the right subfigure (this instance corresponded to the last MCMC sample of our chain that had three large clusters). In addition to the two aforementioned clusters, this assigns the bunched group observations mentioned earlier to their own cluster. Parametric analysis of this dataset typically requires identifying this cluster and treating it as a single observation (Sei et al., 2013), by contrast, our nonparametric approach handles this much more naturally.

Finally, Figure 6 show the log predictive-probabilities of observations given this dataset, with the left subplot giving the distribution of the first component, and the right, the second. The peak of this distribution (the red spot to the right for the first plot, and the spot to the bottom left for the second), correspond to the bunched set of observations mentioned earlier.

## 8 Conclusion

In this paper, we considered the problem of Bayesian inference for the matrix Langevin distribution on the Stiefel manifold. This posterior is doubly intractable, and we proposed and studied a novel exact MCMC algorithm for posterior sampling. We extended our ideas to the nonparametric case, studying the posterior consistency of the resulting model. In our experiments, we applied our ideas to two standard datasets on the Stiefel manifold, besides a few synthetic datasets. Our work represents a first step towards developing more complicated hierarchical models with latent components on the Stiefel manifold. We also hope our ideas are useful to the Bayesian analysis of other, more complicated manifolds. There is a growing need for such models with the increased availability of high-dimensional data with complex, nonlinear structure.

## 9 Acknowledgement

This work was supported by grant R01ES017240 from the National Institute of Environmental Health Sciences (NIEHS) of the National Institute of Health (NIH).

## A Gradient information

Given  $n$  observations  $X_1, \dots, X_n$  with latent variable sets  $\mathcal{Y}_1, \dots, \mathcal{Y}_n$ , let  $N = n + \sum_{i=1}^n |\mathcal{Y}_i|$ , and  $S = \sum_{i=1}^n (X_i + \sum_{j=1}^{|\mathcal{Y}_i|} Y_{i,j})$ . The log joint probability is

$$\begin{aligned} \log(P(\{X_i, \mathcal{Y}_i\})) &= \text{trace}(G^T \boldsymbol{\kappa} S) + \sum_{i=1}^n \sum_{j=1}^{|\mathcal{Y}_i|} (\log(D(\boldsymbol{\kappa}) - D(Y_{i,j}, \boldsymbol{\kappa})) \\ &\quad - \log(D(Y_{i,j}, \boldsymbol{\kappa}))) - N \log(D(\boldsymbol{\kappa})) \end{aligned} \quad (35)$$

Noting that  $D(Y, \boldsymbol{\kappa}) = \left\{ C \prod_{r=1}^p \frac{I_{(d-r-1)/2}(\|\kappa_r N_r^T G_r\|)}{\|\kappa_r N_r^T G_r\|^{(d-r-1)/2}} \right\} := C \tilde{D}(Y, \boldsymbol{\kappa})$ , and that  $\frac{d}{dx}(x^{-m} I_m(x)) = x^{-m} I_{m+1}(x)$ , we have

$$\frac{d\tilde{D}(Y, \boldsymbol{\kappa})}{d\kappa_j} = N_j^T G_j \tilde{D}(Y, \boldsymbol{\kappa}) \frac{I_{(d-j+1)/2}}{I_{(d-j-1)/2}}(\kappa_j N_j^T G_j) \quad \text{and} \quad (36)$$

$$\frac{d\tilde{D}(\boldsymbol{\kappa})}{d\kappa_j} = \tilde{D}(\boldsymbol{\kappa}) \frac{I_{(d-j+1)/2}}{I_{(d-j-1)/2}}(\kappa_j). \quad (37)$$

Then, writing  $L = \log(P(\{X_i, \mathcal{Y}_i\}))$ , we have

$$\begin{aligned} \frac{dL}{d\kappa_k} &= G_{[k]}^T S_{[k]} + \sum_{i=1}^n \sum_{j=1}^{|\mathcal{Y}_i|} \left( \frac{\tilde{D}'(\boldsymbol{\kappa}) - \tilde{D}'(Y_{i,j}, \boldsymbol{\kappa})}{\tilde{D}(\boldsymbol{\kappa}) - \tilde{D}(Y_{i,j}, \boldsymbol{\kappa})} - \frac{\tilde{D}'(Y_{i,j}, \boldsymbol{\kappa})}{\tilde{D}(Y_{i,j}, \boldsymbol{\kappa})} \right) - N \frac{\tilde{D}'(\boldsymbol{\kappa})}{\tilde{D}(\boldsymbol{\kappa})} \quad (38) \\ &= G_{[k]}^T S_{[k]} + \sum_{i=1}^n \sum_{j=1}^{|\mathcal{Y}_i|} \left( \frac{\frac{I_{(d-k+1)/2}}{I_{(d-k-1)/2}}(\kappa_k) - N_k^T G_k \frac{I_{(d-k+1)/2}}{I_{(d-k-1)/2}}(\kappa_k N_k^T G_k)}{1 - \frac{\tilde{D}(Y_{i,j}, \boldsymbol{\kappa})}{\tilde{D}(\boldsymbol{\kappa})}} \right) \\ &\quad - N \frac{I_{(d-k+1)/2}}{I_{(d-k-1)/2}}(\kappa_k) \end{aligned} \quad (39)$$

## B Proofs for posterior consistency

Proof of Theorem 6.1.

*Proof.* The main ideas of proving consistency (from Schwarz, 1978) are to bound the numerator of equation (33) from above and the denominator from below. In order to bound the numerator, we construct uniformly consistent tests which separate the true density from its complement. A condition on the prior mass of the Kullback-Leiber neighborhood of the true density is imposed to lower bound the denominator. For weak consistency, it suffices to check that the prior  $\Pi$  assigns positive mass to any KL neighborhood of  $f_0$  with which one can identify neighborhoods of  $f_0$  for which uniformly consistent tests exist.

By slight abuse of notation, let denote  $f$  as any continuous function on  $\mathcal{M}$  in this proof. From Bhattacharya and Dunson (2012) the following conditions are sufficient to verify that the KL support condition holds.

- (1) The kernel  $g(X, G, \boldsymbol{\kappa})$  is continuous in all of its arguments.
- (2) The set  $\{F_0\} \times D_\epsilon^o$  intersects the support of  $\Pi_1 \times \pi_{\boldsymbol{\kappa}}$  with  $D_\epsilon^o$  as the interior of  $D_\epsilon$ , which is a compact neighborhood of some  $\{\kappa_1, \dots, \kappa_p\}$  in  $\mathbb{R}^p$ .
- (3) For any continuous function  $f$  on  $M$ , there exists a compact neighborhood  $D_\epsilon$  of  $\{\kappa_1, \dots, \kappa_p\}$ , such that

$$\sup_{X \in V_{p,d}, \boldsymbol{\kappa} \in D_\epsilon} \left\| f(X) - \int g(X, G, \boldsymbol{\kappa}) f(G) \lambda(dG) \right\| \leq \epsilon.$$

We first verify condition (1). Note that one can write

$$g(X, G, \boldsymbol{\kappa}) = C(\boldsymbol{\kappa}) \text{etr}(F^T X) = C(\boldsymbol{\kappa}) \exp \left( \sum_{i=1}^p \kappa_i G_{[i]}^T X_{[i]} \right).$$

$g$  is continuous with respect to  $\boldsymbol{\kappa}$  since the hypergeometric function  $C(\boldsymbol{\kappa})$  is continuous and  $\text{etr}(F^T X)$  is clearly continuous with respect to  $\boldsymbol{\kappa}$  as the exponential term can be viewed as a linear combination of  $\kappa_i$ 's.

Now rewrite the density as

$$g(X, G, \boldsymbol{\kappa}) = C(\boldsymbol{\kappa}) \text{etr}(F^T X) = C(\boldsymbol{\kappa}) \exp \left( \frac{p + \sum_{i=1}^p \kappa_i^2 - \rho(F, X)^2}{2} \right),$$

where  $\rho$  is the Frobenius distance between two matrices  $F$  and  $X$ . Therefore  $\text{etr}(F^T X)$  is a continuous density of  $X$  with respect to the Frobenius distance. As mentioned in section 2,  $V_{p,d}$  can be embedded onto the Euclidean space  $M(d, p)$  via the inclusion map. Therefore, one can equip  $V_{p,d}$  with a metric space structure via the extrinsic distance  $\rho$  in the Euclidean space. From the symmetry between  $G$  and  $X$ ,  $g$  is also continuous with respect to  $G$ .

To prove (2), note that DP has weak support on all the measures whose support is contained by the base measure  $P_0$  (See Theorem 3.2.4 in Ghosh and Ramamoorthi (2003), pp. 104). As  $P_0$  and  $\pi_{\boldsymbol{\kappa}}$  have full support, (2) follows immediately.

Let  $I(X) = f(X) - \int g(X, G, \boldsymbol{\kappa}) f(G) \lambda(dG)$ . For the last condition, we must show that there exists some compact subset in  $\mathbb{R}^p$  with non-empty interior,  $D_\epsilon$ , such that

$$\sup_{X \in V_{p,d}, \boldsymbol{\kappa} \in D_\epsilon} \|I(X)\| \leq \epsilon. \quad (40)$$

From symmetry of  $g$  with respect to  $G$  and  $X$ , one can rewrite

$$I(X) = C(\boldsymbol{\kappa}) \int (f(X) - f(G)) \text{etr}(F^T X) \lambda(dG).$$

Let  $\widehat{G} = Q(d)^T G$  where  $Q(d)$  is an orthogonal matrix with first  $p$  columns being  $X$ . Then  $G = Q(d) \widehat{G}$ . As the volume form is invariant under the group action of the orthogonal matrices  $O(d)$  on the left, then one has  $\lambda(dG) = \lambda(d\widehat{G})$ . First note that

$$\rho^2(X, Q(d) \widehat{G}) = \text{Trace} \left( \left( X - Q(d) \widehat{G} \right) \left( X - Q(d) \widehat{G} \right)^T \right)$$

$$\begin{aligned}
&= 2p - 2 \operatorname{Trace} \left( Q(d)^T X \widehat{G}^T \right) \\
&= 2 \sum_{i=1}^p (1 - \widehat{g}_{ii}),
\end{aligned}$$

with  $\widehat{g}_{ii}$  being the diagonal elements of  $\widehat{G}$ . Let  $(1 - \widehat{g}_{ii}) = \frac{1}{\kappa_i} s_{ii}$  for  $i = 1, \dots, p$ , with  $s_{ii} \in [0, 2\kappa_i]$ . Then  $\rho^2(X, Q(d)\widehat{G}) = 2 \sum_{i=1}^p \frac{1}{\kappa_i} s_{ii}$ . As  $\kappa_i \rightarrow \infty$  for all  $i = 1, \dots, p$ ,  $\rho^2(X, Q(d)\widehat{G}) \rightarrow 0$ . Since  $f$  is continuous and the Stiefel manifold is compact, one has for any  $\mathbf{s} = \{s_{11}, \dots, s_{pp}\}$ ,

$$\sup_{X \in V_{p,d}} \left| \left( f(X) - f(Q(d)\widehat{G}) \right) \right| \rightarrow 0, \quad (41)$$

as  $\kappa_i \rightarrow \infty$  for all  $i = 1, \dots, p$ . Let  $\widehat{F}$  be the matrix whose  $k$ th column is  $\kappa_k Q(d)\widehat{G}_{[:,k]}$ . One has

$$\begin{aligned}
\sup_{X \in V_{p,d}} |I(X)| &\leq \sup_{X \in V_{p,d}} C(\boldsymbol{\kappa}) \int \left| \left( f(X) - f(Q(d)\widehat{G}) \right) \right| \operatorname{etr}(\widehat{F}^T X) \lambda(d\widehat{G}) \\
&\leq C(\boldsymbol{\kappa}) \int \left\{ \sup_{X \in V_{p,d}} \left| \left( f(X) - f(Q(d)\widehat{G}) \right) \right| \right\} \exp \left( \sum_{i=1}^p \kappa_i \widehat{g}_{ii} \right) \lambda(d\widehat{G}) \\
&= C(\boldsymbol{\kappa}) \exp \left( \sum_{i=1}^p \kappa_i \right) \int \left\{ \sup_{X \in V_{p,d}} \left| \left( f(X) - f(Q(d)\widehat{G}) \right) \right| \right\} \exp \left( - \sum_{i=1}^p s_{ii} \right) \lambda(d\widehat{G}).
\end{aligned} \quad (42)$$

Let  $\pi_1$  be the transformation given by  $\pi_1(\widehat{g}_{ij}) = \widehat{g}_{ij}$  when  $i \neq j$  and  $\pi_1(\widehat{g}_{ii}) = s_{ii} = \kappa_i(1 - \widehat{g}_{ii})$ . Denote  $\pi_2$  as the transformation of  $\widehat{G}$  given by  $\pi_2(\widehat{g}_{ii}) = (1 - \widehat{g}_{ii})$  and  $\pi_2(\widehat{g}_{ij}) = \widehat{g}_{ij}$  when  $i \neq j$ . Let  $J_1$  and  $J_2$  be the Jacobian corresponding to  $\pi_1^{-1}$  and  $\pi_2^{-1}$  respectively. Denote  $\lambda(d\widehat{G}_s)$  as new volume measure after changing of variables with respect to  $\pi_1$ . Rewrite  $\lambda(d\widehat{G}) = \varphi(\widehat{G}) d\widehat{g}_{11} \wedge d\widehat{g}_{12} \cdots \wedge d\widehat{g}_{dp}$  where  $\varphi(\widehat{G})$  is some function of  $\widehat{G}$ . Then  $\lambda(d\widehat{G}_s)$  is given by the pullback of  $\lambda(d\widehat{G})$  induced by the map  $\pi_1^{-1}$ , that is

$$\lambda(d\widehat{G}_s) = (\pi_1^{-1})^*(\lambda(d\widehat{G})) = \varphi(\pi_1^{-1}(\widehat{G}_s)) \det(J_1) ds_{11} \wedge ds_{12} \cdots \wedge ds_{dp}, \quad (43)$$

where  $s_{ij}$  is the  $(i, j)$ th element of  $\widehat{G}_s$ . Thus

$$\lambda(d\widehat{G}_s) = \varphi(\pi_1^{-1}(\widehat{G}_s)) \det(J_1) \det(J_2) \prod_{i=1}^p \kappa_i d\widehat{g}_{11} \wedge d\widehat{g}_{12} \cdots \wedge d\widehat{g}_{dp}, \quad (44)$$

which implies

$$\lambda(d\widehat{G}) = 1 / \prod_{i=1}^p \kappa_i \frac{1}{\det(J_1) \det(J_2)} \lambda(dG_s). \quad (45)$$

Then the last term of (42) becomes

$$C(\boldsymbol{\kappa}) \exp \left( \sum_{i=1}^p \kappa_i \right) \prod_{i=1}^p \frac{1}{\kappa_i} \int \left\{ \sup_{X \in V_{p,d}} \left| (f(X) - f(Q(d)\widehat{G})) \right| \right\} \times \\ \exp \left( \sum_{i=1}^p -s_{ii} \right) \frac{1}{\det(J_1) \det(J_2)} \lambda(d\widehat{G}_s). \quad (46)$$

It is not hard to see that

$$\int \exp \left( - \sum_{i=1}^p s_{ii} \right) \frac{1}{\det(J_1) \det(J_2)} \lambda(d\widehat{G}_s) < \infty. \quad (47)$$

We now proceed to show that even as  $\kappa_i \rightarrow \infty$ ,

$$C(\boldsymbol{\kappa}) \exp \left( \sum_{i=1}^p \kappa_i \right) \prod_{i=1}^p \frac{1}{\kappa_i} < \infty. \quad (48)$$

One has

$$C(\boldsymbol{\kappa}) \exp \left( \sum_{i=1}^p \kappa_i \right) \prod_{i=1}^p \frac{1}{\kappa_i} = \frac{\prod_{i=1}^p \frac{1}{\kappa_i}}{{}_0F_1 \left( \frac{1}{2}d, \frac{1}{4} \text{Diag} \{ \kappa_1^2, \dots, \kappa_p^2 \} \right) / \prod_{i=1}^p \exp(\kappa_i)}.$$

Write (see Butler and Wood (2003))

$${}_0F_1 \left( \frac{1}{2}d, \frac{1}{4} \text{Diag} \{ \kappa_1^2, \dots, \kappa_p^2 \} \right) = \int_{O_p} \text{etr}(\text{Diag} \{ \kappa_1, \dots, \kappa_p \} T) dT \quad (49)$$

with  $T \in O_p$  the group of all the  $p$  by  $p$  orthogonal matrices with  $dT$  given by  $\wedge_{i < j} t_j^T dt_i$ . When  $\kappa_i \geq 1$  for  $i = 1, \dots, p$ , one looks at

$$\int_{O_p} \frac{\text{etr}(\text{Diag} \{ \kappa_1, \dots, \kappa_p \} T)}{\prod_{i=1}^p \exp(\kappa_i)} dT = \int_{O_p} \exp \left( - \left( \sum_{i=1}^p \kappa_i (1 - t_{ii}) \right) \right) dT,$$

where  $t_{ii}$  are the diagonal elements of  $T$ . Let  $u_{ii} = \kappa_i(1 - t_{ii})$ , one has  $u_{ii} \in [0, 2\kappa_i]$ . Let  $d\widehat{T}$  be the volume form after changing of variable. By the same argument given in (45), we have

$$\int_{O_p} \exp \left( - \left( \sum_{i=1}^p \kappa_i (1 - t_{ii}) \right) \right) dT = \prod_{i=1}^p 1/\kappa_i \int \exp \left( - \left( \sum_{i=1}^p u_{ii} \right) \right) \frac{1}{\det(J_3) \det(J_4)} d\widehat{T},$$

where  $\det(J_3)$  and  $\det(J_4)$  corresponding to determinants of the Jacobian of maps  $\pi_3$  and  $\pi_4$  which are essentially the same maps as  $\pi_1$  and  $\pi_2$  but with domain  $T \in O_p$ . Note



$\int \exp(-(\sum_{i=1}^p u_{ii})) \frac{1}{\det(J_3)\det(J_4)} d\widehat{T}$  is bounded away from zero and infinity as  $\kappa_i \rightarrow \infty$ . Therefore, we can conclude

$$C(\boldsymbol{\kappa}) \exp\left(\sum_{i=1}^p \kappa_i\right) \prod_{i=1}^p \frac{1}{\kappa_i} < \infty. \quad (50)$$

Therefore, combining (41) and (50) and by the dominated convergence theorem, one has

$$\sup_{X \in V_{p,d}} |I(X)| \rightarrow 0$$

as  $\kappa_i \rightarrow \infty$  for all  $i = 1, \dots, p$ . Thus for all  $\epsilon > 0$ , there exists  $M_i$  large enough such that, when  $\kappa_i > M_i$ ,  $\sup_{X \in V_{p,d}} |I(X)| \leq \epsilon$ . One can take  $D_\epsilon$  to be a  $\epsilon$  neighborhood of  $\{\kappa_1, \dots, \kappa_p\}$  with  $\kappa_i > \max\{M_i, i = 1, \dots, p\}$ .  $\square$

Proof of Theorem 6.2.

*Proof.* In order to establish strong consistency, it is not sufficient for the prior  $\Pi$  to assign positive mass to any Kullback-Leibler neighborhood of  $f_0$ . We need to construct high mass sieves with metric entropy  $N(\epsilon, \mathcal{F})$  bounded by certain order where  $N(\epsilon, \mathcal{F})$  is defined as the logarithm of the minimum number of balls with Hellinger radius  $\epsilon$  to cover the space  $\mathcal{F}$ . We refer to Barron et al. (1996) for some general strong consistency theorems. We first proceed to verify the following two conditions on the kernel  $g(X, G, \boldsymbol{\kappa})$ .

- (a) There exists positive constants  $k_0$ ,  $a_1$  and  $A_1$  such that for all  $k > k_0$ ,  $G_1, G_2 \in V_{p,d}$  one has

$$\sup_{X \in V_{p,d}, \boldsymbol{\kappa} \in \phi^{-1}[0,k]} |g(X, G_1, \boldsymbol{\kappa}) - g(X, G_2, \boldsymbol{\kappa})| \leq A_1 k^{a_1} \rho(G_1, G_2), \quad (51)$$

where  $\phi : \mathbb{R}^p \rightarrow [0, \infty)$  is some continuous function of  $\boldsymbol{\kappa}$ .

- (b) There exists positive constants  $a_2$  and  $A_2$  such that for all  $\boldsymbol{\kappa}, \tilde{\boldsymbol{\kappa}} \in \phi^{-1}[0, k]$ ,  $k \geq k_0$ ,

$$\sup_{X, G \in V_{p,d}} |g(X, G, \boldsymbol{\kappa}) - g(X, G, \tilde{\boldsymbol{\kappa}})| \leq A_2 k^{a_2} \rho_2(\boldsymbol{\kappa}, \tilde{\boldsymbol{\kappa}}), \quad (52)$$

where  $\rho_2$  is the Euclidean distance  $\|\cdot\|_2$  on  $\mathbb{R}^p$ .

Let  $G_1, G_2 \in V_{p,d}$  and  $F_1$  and  $F_2$  be such that their  $i$ th columns are given by  $\kappa_i G_{1[.,i]}$  and  $\kappa_i G_{2[.,i]}$  respectively. For  $s, t \in [0, c]$  and  $c > 0$ , one has

$$\left| \exp\left(-\frac{s^2}{2}\right) - \exp\left(-\frac{t^2}{2}\right) \right| \leq \left| \eta \exp\left(-\frac{\eta^2}{2}\right) (s - t) \right| \leq c|s - t|,$$

where  $\eta$  is some point between  $s$  and  $t$ . Let  $k_{\max} = \max\{\kappa_1, \dots, \kappa_p\}$ . A little calculation shows that  $\rho(F, X) \leq \sqrt{\sum_{i=1}^p (\kappa_i + 1)^2}$ , so that

$$\sup_{X \in V_{p,d}, \boldsymbol{\kappa} \in \phi^{-1}[0,k]} \left| g(X, G_1, \boldsymbol{\kappa}) - g(X, G_2, \boldsymbol{\kappa}) \right|$$

$$\begin{aligned}
&= \sup_{X \in V_{p,d}, \boldsymbol{\kappa} \in \phi^{-1}[0,k]} \left| C(\boldsymbol{\kappa}) \exp\left(\frac{p}{2}\right) \exp\left(\frac{\sum_{i=1}^p \kappa_i}{2}\right) \left( \exp\left(-\frac{\rho^2(F_1, X)}{2}\right) - \exp\left(-\frac{\rho^2(F_2, X)}{2}\right) \right) \right| \\
&\leq \sup_{X \in V_{p,d}, \boldsymbol{\kappa} \in \phi^{-1}[0,k]} \left| C(\boldsymbol{\kappa}) \exp\left(\frac{p}{2}\right) \exp\left(\frac{\sum_{i=1}^p \kappa_i}{2}\right) \sqrt{\sum_{i=1}^p (\kappa_i + 1)^2} (\rho(F_1, X) - \rho(F_2, X)) \right| \\
&\leq \exp\left(\frac{p}{2}\right) \sup_{X \in V_{p,d}, \boldsymbol{\kappa} \in \phi^{-1}[0,k]} \left| C(\boldsymbol{\kappa}) \exp\left(\frac{\sum_{i=1}^p \kappa_i}{2}\right) \rho(F_1, F_2) \sqrt{\sum_{i=1}^p (\kappa_i + 1)^2} \right| \\
&\leq 2 \exp\left(\frac{p}{2}\right) \sup_{X \in V_{p,d}, \boldsymbol{\kappa} \in \phi^{-1}[0,k]} \left| C(\boldsymbol{\kappa}) \exp\left(\frac{\sum_{i=1}^p \kappa_i}{2}\right) \sqrt{\sum_{i=1}^p \kappa_i^2} \rho(G_1, G_2) \sqrt{\sum_{i=1}^p (\kappa_i + 1)^2} \right| \\
&\leq 2 \exp\left(\frac{p}{2}\right) \sup_{X \in V_{p,d}, \boldsymbol{\kappa} \in \phi^{-1}[0,k]} \left| C \prod_{i=1}^p \kappa_i \sqrt{\sum_{i=1}^p \kappa_i^2} \sqrt{\sum_{i=1}^p (\kappa_i + 1)^2} \rho(G_1, G_2) \right|
\end{aligned}$$

where  $C$  is some constant according to (50). Let  $\phi(\boldsymbol{\kappa}) = \sqrt{\sum_{i=1}^p (\kappa_i + 1)^2}$ . If  $\phi(\boldsymbol{\kappa}) \leq k$ , then  $\sqrt{\sum_{i=1}^p \kappa_i^2} \leq \phi(\boldsymbol{\kappa}) \leq k$  and  $\kappa_i \leq k$  for each  $i$ . Thus  $\prod_{i=1}^p \kappa_i \leq k^p$ . Therefore,

$$\sup_{X \in V_{p,d}, \boldsymbol{\kappa} \in \phi^{-1}[0,k]} |g(X, G_1, \boldsymbol{\kappa}) - g(X, G_2, \boldsymbol{\kappa})| \leq C_1 k^{p+2} \rho(G_1, G_2),$$

with  $C_1$  some constant. Let  $a_1 = p + 2$ , then condition (a) holds.

Let  $\boldsymbol{\kappa}, \tilde{\boldsymbol{\kappa}} \in \mathbb{R}^p$  be two vectors of the concentration parameters. By the mean value theorem, one has for some  $t \in (0, 1)$

$$g(X, G, \boldsymbol{\kappa}) - g(X, G, \tilde{\boldsymbol{\kappa}}) = (\nabla g(X, G, (1-t)\boldsymbol{\kappa} + t\tilde{\boldsymbol{\kappa}})) \cdot (\boldsymbol{\kappa} - \tilde{\boldsymbol{\kappa}}),$$

where  $\nabla g(X, G, (1-t)\boldsymbol{\kappa} + t\tilde{\boldsymbol{\kappa}})$  is the gradient of  $g(X, G, \boldsymbol{\kappa})$  with respect to  $\boldsymbol{\kappa}$  evaluated at  $(1-t)\boldsymbol{\kappa} + t\tilde{\boldsymbol{\kappa}}$  and  $\cdot$  denotes the inner product. By Cauchy-Schwarz inequality, one has

$$|g(X, G, \boldsymbol{\kappa}) - g(X, G, \tilde{\boldsymbol{\kappa}})| \leq \|\nabla g(X, G, (1-t)\boldsymbol{\kappa} + t\tilde{\boldsymbol{\kappa}})\|_2 \|\boldsymbol{\kappa} - \tilde{\boldsymbol{\kappa}}\|_2.$$

Note that for  $i = 1, \dots, p$ ,

$$\begin{aligned}
\frac{\partial g}{\partial \kappa_i} &= \exp\left(-\sum_{i=1}^p \kappa_i (1 - G_{[i]}^T X_{[i]})\right) \left( C(\boldsymbol{\kappa}) G_{[i]}^T X_{[i]} \exp\left(\sum_{i=1}^p \kappa_i\right) + \frac{\partial C(\boldsymbol{\kappa})}{\partial \kappa_i} \exp\left(\sum_{i=1}^p \kappa_i\right) \right) \\
&= \exp\left(-\sum_{i=1}^p \kappa_i (1 - G_{[i]}^T X_{[i]})\right) \left( C(\boldsymbol{\kappa}) G_{[i]}^T X_{[i]} \exp\left(\sum_{i=1}^p \kappa_i\right) \right. \\
&\quad \left. - C^2(\boldsymbol{\kappa}) \frac{\partial_0 F_1\left(\frac{1}{2}d, \frac{1}{4} \text{Diag}\{\kappa_1^2, \dots, \kappa_p^2\}\right)}{\partial \kappa_i} \exp\left(\sum_{i=1}^p \kappa_i\right) \right).
\end{aligned}$$

By applying the general Leibniz rule for differentiation under an integral sign, one has

$$\begin{aligned} \frac{\partial_0 F_1\left(\frac{1}{2}d, \frac{1}{4} \text{Diag}\{\kappa_1^2, \dots, \kappa_p^2\}\right)}{\partial \kappa_i} &= \int_{O_p} \frac{\partial \text{etr}(\text{Diag}\{\kappa_1, \dots, \kappa_p\} S)}{\partial \kappa_i} dS \\ &= \int_{O_p} s_{ii} \exp\left(\sum_{i=1}^p \kappa_i s_{ii}\right) dS \\ &\leq \int_{O_p} \exp\left(\sum_{i=1}^p \kappa_i s_{ii}\right) dS = \frac{1}{C(\boldsymbol{\kappa})}. \end{aligned}$$

Then one has

$$\begin{aligned} \left| \frac{\partial g(X, G, \boldsymbol{\kappa})}{\partial \kappa_i} \right| &\leq C(\boldsymbol{\kappa}) \exp\left(\sum_{i=1}^p \kappa_i\right) + C^2(\boldsymbol{\kappa}) \frac{\partial_0 F_1\left(\frac{1}{2}d, \frac{1}{4} \text{Diag}\{\kappa_1^2, \dots, \kappa_p^2\}\right)}{\partial \kappa_i} \exp\left(\sum_{i=1}^p \kappa_i\right) \\ &\leq 2C(\boldsymbol{\kappa}) \exp\left(\sum_{i=1}^p \kappa_i\right) \leq C_2 \prod_{i=1}^p \kappa_i, \end{aligned}$$

for some constant  $C_2$  by (50). Therefore,

$$\|\nabla g(X, G, (1-t)\boldsymbol{\kappa} + t\tilde{\boldsymbol{\kappa}})\|_2 \leq C_2 k^p.$$

Then one has

$$|g(X, G, \boldsymbol{\kappa}) - g(X, G, \tilde{\boldsymbol{\kappa}})| \leq C_2 k^p \|\boldsymbol{\kappa} - \tilde{\boldsymbol{\kappa}}\|_2.$$

Letting  $a_2 = p$ , condition (b) is verified.

We proceed to verify the two following entropy conditions:

- (c) For any  $k \geq k_0$ , the subset  $\phi^{-1}[0, k]$  is compact and its  $\epsilon$ -covering number is bounded by  $(k\epsilon^{-1})^{b_2}$  for some constant  $b_2$  independent of  $\boldsymbol{\kappa}$  and  $\epsilon$ .
- (d) The  $\epsilon$  covering number of the manifold  $V_{p,d}$  is bounded by  $A_3 \epsilon^{-a_3}$  for any  $\epsilon > 0$ .

It is easy to verify condition (c) as  $\phi^{-1}([0, k]) = \{\boldsymbol{\kappa}, \sum_{i=1}^p (\kappa_i + 1)^2 \leq k^2\}$ , which is a subset of a shifted Euclidean ball in  $\mathbb{R}^p$  with radius  $k$ . With a direct argument using packing numbers (Pollard, 1990, see Section 4), one can obtain a bound for the entropy of  $\phi^{-1}[0, k]$  which is given by  $\frac{3k^p}{\epsilon^p}$ . Thus condition (c) holds with  $b_2 = p$ .

Denote  $N(\epsilon)$  as the entropy of  $V_{p,d}$  and  $N_E(\epsilon)$  as the entropy of  $V_{p,d}$  viewed as a subset of  $\mathbb{R}^{pd}$  (thus points covering  $V_{p,d}$  do not necessarily lie on  $V_{p,d}$  for the latter case). One can show that  $N(2\epsilon) \leq N_E(\epsilon)$ . Note that  $V_{p,d} \subset [-1, 1]^{pd}$  which is a subset of a Euclidean ball of radius  $\sqrt{dp}$  centered at zero, the  $\epsilon$  number of which is bounded  $\left(\frac{3\sqrt{dp}}{\epsilon}\right)^{dp}$ . Therefore, condition (d) holds with  $a_3 = dp$ . Then by Corollary 1 in Bhattacharya and Dunson (2012), strong consistency follows. □

# C Posterior sampling for the Dirichlet process extension

## C.1 Inference for the nonparametric model:

Extending our ideas from Section 4 to the nonparametric case involves adapting existing DP sampling techniques to doubly-intractable mixture components. MCMC sampling algorithms for the DP can broadly be classified into two kinds: marginal samplers (based on the Chinese restaurant process (CRP) representation of the DP) (Neal, 2000), and conditional samplers based on the stick-breaking representation (Ishwaran and James, 2001). Here, we focus on the former, although it should be clear how similar ideas apply to the latter.

The Chinese restaurant process describes the distribution over partitions of observations that results from integrating out the DP-distributed discrete random probability measure  $\Pi$ . For a CRP-based sampler, at any iteration, the state of the sampler consists of a partitioning of the data (represented by an assignment of each observation to a latent component), and the parameters associated with each cluster. Let  $n$  be the number of observations, and let these be partitioned into  $k$  clusters. The cluster assignments of the observations are represented by an  $n$ -component vector  $\mathbf{c}$ , with  $c_i$  taking values in  $\{1, \dots, k\}$ . The MCMC sampler proceeds by repeating two steps:

### C.1.1 Update the cluster assignments of the observations

We perform this step by sweeping through the observations, conditionally updating the cluster assignment of each observation based on the CRP sampling rule. In particular, from the exchangeability of observations, we treat the current observation as the last one, so that *a priori*, its probability of joining cluster  $c$  (resp. a new cluster) is proportional to  $n_c$  (resp.  $\alpha$ ). Here  $n_c$  is the number of observations associated with cluster  $c$ , and  $\alpha$  is the DP concentration parameter. Letting cluster  $c$  have parameters  $(G_c^*, \kappa_c^*)$ , the likelihood for observation  $X_i$  is  $\text{etr}(X_i^T F_c^*)/Z(F_c^*)$ . Thus, we have for observation  $i$ :

$$P(c_i = c|\cdot) \propto n_c \text{etr}(X_i^T F_c^*)/Z(F_c^*) \quad c \leq k \quad (53)$$

$$P(c_i = k + 1|\cdot) \propto \alpha \int_{V_{p,d}} \frac{\text{etr}(X_i^T F^*)}{Z(F^*)} P(F^*) \lambda(dG^*) d\kappa^*. \quad (54)$$

Implementing this requires overcoming two problems. One is that the lack of conjugacy make the integral in equation (54) intractable. A standard approach (Algorithm 8 in Neal (2010)) is to first assign the new cluster a parameter drawn from the prior, and then assign observation  $i$  to a cluster. By instantiating the parameter associated with the new cluster, we avoid having to solve the integral of equation (54). To improve this proposal, one can consider  $\zeta$  candidate new clusters (for some integer  $\zeta \geq 1$ ), assigning each a parameter drawn from the prior. Now, the probability of joining a new cluster  $z \in \{1, \dots, \zeta\}$  is given by  $\frac{\alpha}{\zeta} \text{etr}(X_i^T F_z^*)/Z(F_z^*)$ . For more details, we refer to Neal (2010).

The second issue is more unique to our problem, and concerns the fact that even given the cluster parameters, the probability of assignment involves the normalization constant  $Z(F^*) = Z(\boldsymbol{\kappa}^*)$  (see equation (53)). For the location mixture model, where all clusters have the same scale parameter  $\boldsymbol{\kappa}$ , this is a common multiplicative factor, and is thus not an issue. For the general location-scale mixture, we can deal with this using similar auxiliary variable schemes as before.

A first approach follows the exchange sampler, proposing to move an observation  $i$  from its current cluster  $c_o$  to a random new cluster  $c_n$  (chosen by some prespecified proposal distribution). This move is then accepted using unbiased estimates of the probabilities in equations (53) and (54). In particular, we generate a new observation  $\hat{X}$  with parameter  $F_{c_n}^*$ , and simultaneously propose moving this from  $c_n$  to  $c_o$ . The acceptance probability is then given by

$$p_{acc} = \frac{n_{c_n} \text{etr}(X_i^T F_{c_n}^*) \text{etr}(\hat{X}^T F_{c_o}^*)}{n_{c_o} \text{etr}(X_i^T F_{c_o}^*) \text{etr}(\hat{X}^T F_{c_n}^*)}. \quad (55)$$

While it is possible to follow and improve this approach, a conceptually much simpler approach builds on the latent variable representation of Section 4.4. Recall that the joint distribution of an observation along with the rejected proposals of the rejection sampling algorithm is tractable ( $P(X_i \cup \mathcal{Y}_i | \boldsymbol{\kappa}, G)$  in equation (22)). Thus, by instantiating these variables, we can calculate the cluster assignment probability as

$$P(c_i = c | \cdot) \propto n_c P(X_i, \mathcal{Y}_i | F_c^*) \quad c \leq k \quad (56)$$

$$P(c_i = k + 1 | \cdot) \propto \alpha \int_{V_{p,d}} P(X_i, \mathcal{Y}_i | F_c^*) \lambda(dG^*) d\boldsymbol{\kappa}^*. \quad (57)$$

To avoid evaluating the integral in the second equation, once again, we use Algorithm 8 from Neal (2010). We have thus reduced the original problem to the standard problem of MCMC sampling for DP mixture models with nonconjugate base measures.

### C.1.2 Update the cluster parameters

We update the parameters associated with each cluster using parametric sampling ideas from section 3. For our experiments, we used the Hamiltonian Monte Carlo sampler, cycling through each cluster and updating its parameters.

## References

- Adams, R. P., Murray, I., and MacKay, D. J. C. (2009). The Gaussian process density sampler. In Koller, D., Schuurmans, D., Bengio, Y., and Bottou, L., editors, *Advances in Neural Information Processing Systems 21*, pages 9–16.
- Andrieu, C. and Roberts, G. O. (2009). The pseudo-marginal approach for efficient Monte Carlo computations. *The Annals of Statistics*, 37(2):697–725.

- Barron, A., Schervish, M., and Wasserman, L. (1996). The consistency of posterior distributions in nonparametric problems. *The Annals of Statistics*, 27:536–561.
- Beskos, A. and Roberts, G. (2005). Exact simulation of diffusions. *The Annals of Applied Probability*, 15(4):2422 – 2444.
- Bhattacharya, A. and Bhattacharya, R. (2012). *Nonparametric Inference on Manifolds: With Applications to Shape Spaces*. IMS monograph series 2. Cambridge University Press.
- Bhattacharya, A. and Dunson, D. (2010). Nonparametric Bayesian density estimation on manifolds with applications to planar shapes. *Biometrika*, 97:851–865.
- Bhattacharya, A. and Dunson, D. (2012). Strong consistency of nonparametric Bayes density estimation on compact metric spaces. *Ann Inst Stat Math.*, 64(4):687–714.
- Butler, R. and Wood, A. (2003). Laplace approximation for Bessel functions of matrix argument. *Journal of Computational and Applied Mathematics*, 155(2):359–382.
- Camano-Garcia, G. (2006). *Statistics on Stiefel manifolds*. PhD thesis, University of Iowa.
- Chikuse, Y. (1993). High dimensional asymptotic expansions for the matrix langevin distributions on the stiefel manifold. *Journal of Multivariate Analysis*, 44(1):82–101.
- Chikuse, Y. (2003a). Concentrated matrix langevin distributions. *Journal of Multivariate Analysis*, 85(2):375 – 394.
- Chikuse, Y. (2003b). *Statistics on Special Manifolds*. Springer, New York.
- Chikuse, Y. (2006). State space models on special manifolds. *Journal of Multivariate Analysis*, 97(6):1284 – 1294.
- Downs, T., Liebman, J., and Mackay, W. (1971a). Statistical methods for vectorcardiogram orientations. In *Vectorcardiography 2: Proc. XIth International Symposium on Vectorcardiography (I. Hoffman, R.I. Hamby and E. Glassman, Eds.)*, pages 216–222. North-Holland, Amsterdam.
- Downs, T. D., Liebman, J., and Mackay, W. (1971b). Statistical methods for vectorcardiogram orientations. In *Vectorcardiography 2: Proc. XIth International Symposium on Vectorcardiography*.
- Edelman, A., Arias, T., and Smith, S. T. (1998). The geometry of algorithms with orthogonality constraints. *SIAM J. Matrix Anal. Appl.*, 20(2):303–353.
- Ferguson, T. S. (1973). A Bayesian analysis of some nonparametric problems. *The Annals of Statistics*, 1(2):209–230.
- Ghosh, J. and Ramamoorthi, R. (2003). *Bayesian Nonparametrics*. Springer, New York.

- Hoff, P. (2009a). A hierarchical eigenmodel for pooled covariance estimation. *Journal of the Royal Statistical Society, Series B: Statistical Methodology*, 71(5):971–992.
- Hoff, P. D. (2009b). Simulation of the Matrix Bingham-von Mises-Fisher Distribution, with Applications to Multivariate and Relational Data. *Journal of Computational and Graphical Statistics*, 18(2):438–456.
- Hoff, P. D. (2013). Bayesian analysis of matrix data with rstiefel.
- Hornik, K. and Grn, B. (2013). On conjugate families and Jeffreys priors for von Mises Fisher distributions . *Journal of Statistical Planning and Inference*, 143(5):992 – 999.
- Ishwaran, H. and James, L. F. (2001). Gibbs sampling methods for stick-breaking priors. *Journal of the American Statistical Association*, 96(453):161–173.
- Khatri, C. G. and Mardia, K. V. (1977). The Von Mises-Fisher Matrix Distribution in Orientation Statistics. *Journal of the Royal Statistical Society. Series B (Methodological)*, 39(1).
- Moller, J., Pettitt, A. N., Reeves, R., and Berthelsen, K. K. (2006). An efficient markov chain monte carlo method for distributions with intractable normalising constants. *Biometrika*, 93(2):451–458.
- Muirhead, R. J. (2005). *Aspects of Multivariate Statistical Theory*. Wiley-Interscience.
- Murray, I., Ghahramani, Z., and MacKay, D. J. C. (2006). MCMC for doubly-intractable distributions. In *Proceedings of the 22nd Annual Conference on Uncertainty in Artificial Intelligence (UAI-06)*, pages 359–366. AUAI Press.
- Neal, R. M. (2000). Markov chain sampling methods for Dirichlet process mixture models. *Journal of Computational and Graphical Statistics*, 9:249–265.
- Neal, R. M. (2010). MCMC using Hamiltonian dynamics. *Handbook of Markov Chain Monte Carlo*, 54:113–162.
- Plummer, M., Best, N., Cowles, K., and Vines, K. (2006). CODA: Convergence diagnosis and output analysis for MCMC. *R News*, 6(1):7–11.
- Pollard, D. (1990). *Empirical processes: theory and applications*, volume 2. NSF-CBMS Regional Conference Series in Probability and Statistics.
- Schwarz, G. (1978). Estimation the dimension of a model. *The Annals of Statistics*, 6(2):461–464.
- Sei, T., Shibata, H., Takemura, A., Ohara, K., and Takayama, N. (2013). Properties and applications of Fisher distribution on the rotation group. *Journal of Multivariate Analysis*, 116(0):440 – 455.

- Walker, S. G. (2011). Posterior sampling when the normalizing constant is unknown. *Communications in Statistics - Simulation and Computation*, 40(5):784–792.
- Wood, A. T. (1994). Simulation of the von Mises Fisher distribution. *Communications in Statistics-Simulation and Computation*, 23(1):157–164.